iScience

CellPress
OPEN ACCESS

Article

Sustained type I interferon signaling after human immunodeficiency virus type 1 infection of human iPSC derived microglia and cerebral organoids

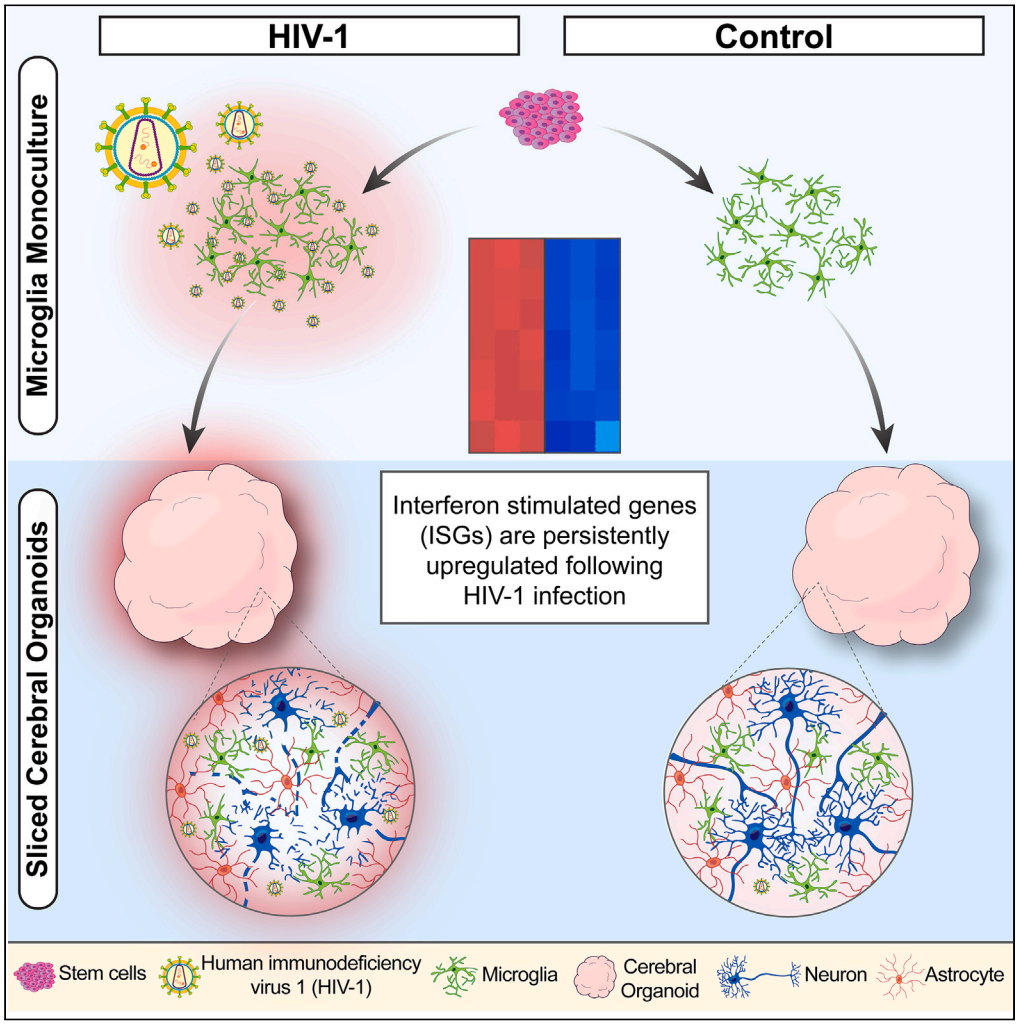

Andrew J. Boreland, Alessandro C. Stillitano, Hsin-Ching Lin, ..., Peng Jiang, Zhiping P. Pang, Arnold B. Rabson

zhiping.pang@rutgers.edu (Z.P.P.)
rabsonab@rwjms.rutgers.edu (A.B.R.)

Highlights

HIV-1 productively infects iPSC-derived microglia and triggers inflammatory activation

HIV-1 infection of microglia results in sustained type I interferon signaling

Type I interferon signaling persists in HIV-1-infected sliced cerebral organoids

Boreland et al., iScience 27, 109628
May 17, 2024
https://doi.org/10.1016/j.isci.2024.109628

iScience

CellPress
OPEN ACCESS

Article

Sustained type I interferon signaling after human immunodeficiency virus type 1 infection of human iPSC derived microglia and cerebral organoids

Andrew J. Boreland,[1,2] Alessandro C. Stillitano,[1] Hsin-Ching Lin,[1] Yara Abbo,[1] Ronald P. Hart,[3] Peng Jiang,[3] Zhiping P. Pang,[1,2,*] and Arnold B. Rabson[1,4,5,*]

SUMMARY

Human immunodeficiency virus type-1 (HIV-1)-associated neurocognitive disorder (HAND) affects up to half of people living with HIV-1 and causes long term neurological consequences. The pathophysiology of HIV-1-induced glial and neuronal functional deficits in humans remains enigmatic. To bridge this gap, we established a model simulating HIV-1 infection in the central nervous system using human induced pluripotent stem cell (iPSC)-derived microglia combined with sliced neocortical organoids. Incubation of microglia with two replication-competent macrophage-tropic HIV-1 strains (JRFL and YU2) elicited productive infection and inflammatory activation. RNA sequencing revealed significant and sustained activation of type I interferon signaling pathways. Incorporating microglia into sliced neocortical organoids extended the effects of aberrant type I interferon signaling in a human neural context. Collectively, our results illuminate a role for persistent type I interferon signaling in HIV-1-infected microglia in a human neural model, suggesting its potential significance in the pathogenesis of HAND.

INTRODUCTION

The global burden of human immunodeficiency virus-1 (HIV-1) infection remains profound, with neurocognitive complications manifesting in a significant proportion of infected individuals despite the remarkable success of combined antiretroviral therapy (cART) in reducing morbidity and mortality. Up to 55% of people living with HIV-1 experience neurological complications that may develop into HIV-associated neurocognitive disorder (HAND).[1–4] This debilitating disorder manifests across a spectrum of cognitive, motor, affective, and behavioral impairments, which can severely impact the quality of life for affected individuals, emphasizing an urgent need for a better understanding of its underlying mechanisms.[5,6] The etiology and neuropathogenesis of HAND remain enigmatic, as there has been no evidence of neuronal HIV-1 infection. Decades of research suggest that HAND development is caused by a combination of both direct and indirect effects involving viral proteins, inflammatory cytokines and chemokines, and dysregulated neuroimmune interactions.[7–14] Interestingly, clinical symptoms of HAND correlate more closely with cytokine production, neuronal pathology, decreased synaptic density, and increased microglia than with central nervous system (CNS) viral load.[15,16] Currently there is a lack of mechanistic understanding due to a need for better experimental models that can address these questions, especially regarding neuroimmune interactions.

A pivotal component of neuroimmune interactions is the innate immune response, including the production and signaling of interferons, which have recently been implicated in the neuropathology of various neurological diseases (reviewed by Hofer and Campbell[17] and McGlasson et al.[18]). Interferons and their downstream signaling through interferon stimulated genes (ISGs) are primarily an innate immune response to viral infection (reviewed by Platanias[19]). However, recent literature suggests a role for dysregulated type I interferon signaling in neurological diseases such as Alzheimer's disease (AD),[20,21] COVID-19-related brain fog,[22,23] aging-associated dementia,[24] and HIV-associated dementia.[25–29] Clinically, type I interferons have been shown to be a driver of cognitive impairment both in diseased states and when administered exogenously.[30] Indeed, many studies using interferon treatment for various severe cancers and chronic viral hepatitis C have reported that patients receiving interferon-alpha displayed cognitive, mood, and behavioral deficits that arose and worsened with prolonged, multi-week treatment regimens.[31–36] Taken together, these studies indicate a role for aberrant type I interferon signaling in compromising neuronal and glial function, leading to cognitive deficits and degeneration.

Microglia, as the resident immune cells of the CNS and the primary CNS target of HIV-1 infection, contribute significantly to the pathophysiology of HAND, largely through their secretory and functional dysregulation. Under homeostatic conditions, microglia play important

[1]Child Health Institute of New Jersey, Rutgers Robert Wood Johnson Medical School, New Brunswick, NJ 08901, USA
[2]Department of Neuroscience and Cell Biology, Rutgers Robert Wood Johnson Medical School, New Brunswick, NJ 08854, USA
[3]Department of Cell Biology and Neuroscience, Rutgers University, Piscataway, NJ 08854, USA
[4]Departments of Pharmacology, Pathology & Laboratory Medicine, and Pediatrics, Rutgers Robert Wood Johnson Medical School, New Brunswick, NJ 08901, USA
[5]Lead contact
*Correspondence: zhiping.pang@rutgers.edu (Z.P.P.), rabsonab@rwjms.rutgers.edu (A.B.R.)
https://doi.org/10.1016/j.isci.2024.109628

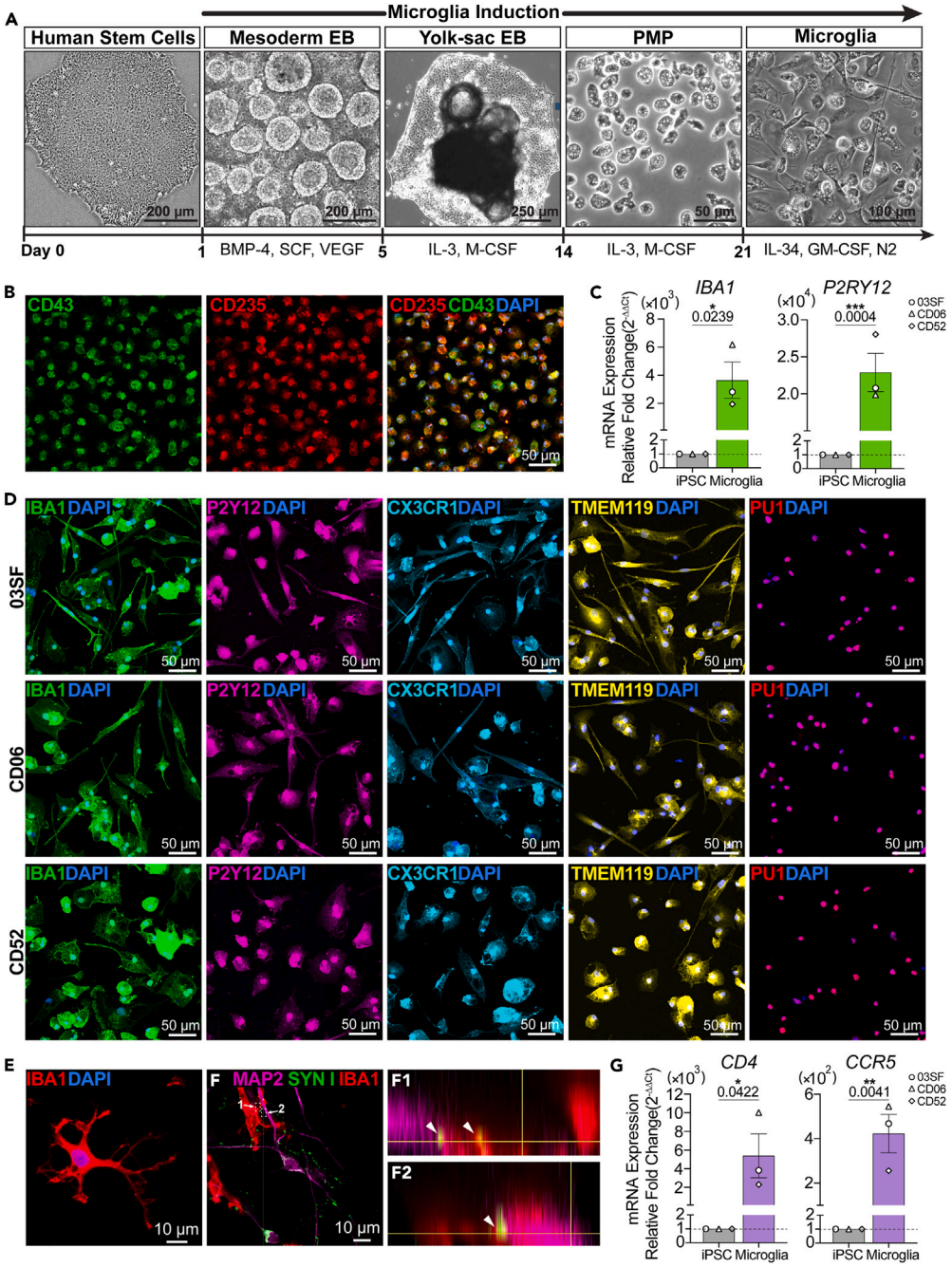

Figure 1. Human microglia are efficiently generated from induced pluripotent stem cells

(A) Representative brightfield images showing the induction of iPSCs to mesodermal yolk sac embryoid bodies (EB) and then to primitive microglia progenitor cells (PMPs) and microglia. Scale bars, 200 µm or 250 µm or 50 µm or 100 µm as indicated.

(B) Representative confocal images of PMPs expressing the yolk sac marker CD235 and the hematopoietic progenitor cell marker CD43 in the 03SF cell line. Scale bars, 50 µm.

(C) RT-qPCR analysis of *IBA1* and *P2RY12* mRNA expression in iPSCs and iPSC-derived microglia; $n = 3$ cell lines (03SF, CD06, and CD52); One-tailed t test; $*p < 0.05$, $***p < 0.001$; data are presented as the mean ± SEM.

(D) Representative confocal images of microglia stained for the microglial markers IBA1, P2Y12, CX3CR1, TMEM119, and PU1 and costained with DAPI; $n = 3$ cell lines (03SF, CD06, and CD52). Scale bars, 50 µm.

(E) Representative confocal image of a microglial cell displaying ramified morphology after 4 weeks of coculture with neurons. Scale bars, 10 µm.

Figure 1. *Continued*

(F) Representative confocal images of a 03SF cell line iPSC-derived microglial neuronal coculture stained for neurons (MAP2), synapses (SYN1), and microglia (IBA1). (F1 and F2) Orthogonal view of microglial (IBA1+) processes colocalized with neuronal dendrites (MAP2) and synapses (SYN1). Scale bars, 10 μm.
(G) RT-qPCR analysis of *CD4* and *CCR5* mRNA from iPSCs and microglia; $n = 3$ cell lines (03SF, CD06, and CD52); One-tailed t test; $^{*}p < 0.05$, $^{**}p < 0.01$; data are presented as the mean ± SEM.

roles in synaptic pruning, phagocytic functions, immune surveillance, and extracellular matrix remodeling.[37,38] When challenged, microglial activation can be either neurotoxic, producing proinflammatory cytokines and chemokines, or neurotrophic, producing anti-inflammatory cytokines.[39] Microglia exhibit a heterogeneous spectrum of activation and disease-associated states with unique properties and consequences on neuronal functions.[40–42]

Since HIV-1 specifically infects humans, the ability of traditional animal model organisms to replicate the complex disease processes of HAND is inherently limited. HIV-1-Simian immunodeficiency virus chimeras (SHIVs) have been studied in monkey models. However, these models are limited in their availability and utility for molecular analyses [reviewed by Byrnes et al.[43] and Moretti et al.[44]]. Recent advances in stem cell technologies have opened up new possibilities for modeling and studying HAND, particularly through the development of human iPSC-derived neurons, astrocytes, and microglia capable of mimicking complex *in vivo* neuroimmune interactions when grown in three dimensional cerebral organoid cultures.[45–47] Cerebral organoids offer a powerful and physiologically relevant platform to study complex neuroimmune interactions, but traditional organoid differentiation protocols do not produce microglia. Recent studies have demonstrated the feasibility of infecting iPSC-derived macrophages[48] and microglia[49] with HIV-1. Moreover, these infected microglia have been effectively cocultured in various model systems, including human stem cell-derived neural tricultures,[14,50] primary neuron progenitor cell-derived organoids,[51] iPSC-derived cerebral organoids,[52] and a humanized mouse model.[53]

In this study, we hypothesized that by infecting iPSC-derived microglia with replication competent HIV-1 and integrating them into sliced neocortical organoids, we could recapitulate neuroimmune dysregulation related to HAND pathology. We demonstrate that HIV-1 infection of iPSC-derived microglia leads to persistent activation of type I interferon signaling and microglial activation in both microglial monocultures and in the context of cerebral organoids.

RESULTS

Human microglia are efficiently generated from iPSCs

To induce microglial differentiation, we used three iPSC lines (Table S1) and employed previously published protocols.[47,54] To mimic *in vivo* microglial development from the yolk sac, iPSC embryoid bodies were patterned toward a mesodermal yolk sac lineage that generates primitive macrophage precursors (PMPs) after 3 weeks of culture (Figure 1A). The identity of the PMPs was confirmed by immunocytochemistry against CD235, a marker for yolk sac,[55] and CD43, a marker for hematopoietic progenitor like cells[56] (Figure 1B). Upon further maturation under the influence of a colony stimulating factor 1 receptor (CSF1R) antagonist, interleukin 34 (IL-34), and granulocyte maturation factor (GM-CSF), PMPs exhibit a more pronounced microglial phenotype. This was evidenced by a significant increase in mRNA expression of the microglial markers ionized calcium binding molecule 1 (*IBA1*) and purinergic receptor *P2RY12* across all three cell lines (Figure 1C, biological replicates of each cell line shown in Figure S1). Supporting these gene expression results, we noted robust immunocytochemical staining of the microglial markers IBA1, P2Y12, CX3CR1, transmembrane protein 119 (TMEM119), and transcription factor PU.1 in maturing microglia from these same lines (Figure 1D). Upon coculture of microglia with iPSC-derived neurons,[47] we found that microglia display a more elaborate morphology (Figure 1E). Furthermore, costaining with the neuronal dendritic marker microtubule-associated protein 2 (MAP2) and the presynaptic marker synapsin 1 (SYN1) revealed that microglial processes interact with dendrites and colocalize with synaptic puncta, indicating putative microglia-synapse interactions (Figure 1F).

Given the tropism of HIV-1 for CD4 receptor expressing cells and the requirement of CCR5 coreceptor expression for infection of monocyte/macrophage related cell lineages, we assessed the gene expression of *CD4* and *CCR5* in iPSC-derived microglia. Results showed significantly increased mRNA expression of *CD4* and *CCR5* in microglia differentiated from all three iPSC lines (Figure 1G, biological replicates of each cell line shown in Figure S1) (Table S2). These results demonstrate that microglia can be successfully and reproducibly generated from iPSCs. Crucially, these cells express appropriate markers for microglial identity and infection by HIV-1.

iPSC-derived microglia are productively infected by HIV-1 and exhibit inflammatory activation

Having confirmed the generation and maturation of iPSC-derived microglia, we next determined whether these cells could sustain a productive infection by replication competent, macrophage tropic HIV-1. To this end, we incubated male 03SF iPSC-derived microglia with JRFL HIV (2 ng/mL), an R5 tropic HIV-1 strain isolated from the cerebral spinal fluid (CSF) of a patient with severe HAND.[57,58] Compared to uninfected controls, HIV-1-infected microglia robustly expressed HIV-1 *gag/pol* RNA within 6–9 days after infection[59] (Figure 2A). As a key indicator of productive HIV-1 infection, the production of secreted p24 was measured.[60,61] Using ELISA to detect secreted p24 in the culture supernatant, we observed increased protein production starting 1 week post infection, peaking around day 16, and then maintaining consistent levels for more than 2 weeks (Figure 2B). Finally, we found that after just 4 days post infection, polymerase chain reaction (PCR) products spanning the junction of the two long terminal repeats (LTR) of HIV DNA circles were detected in HIV-1 incubated cultures indicating the presence of active viral replication[62] (Figure S2).

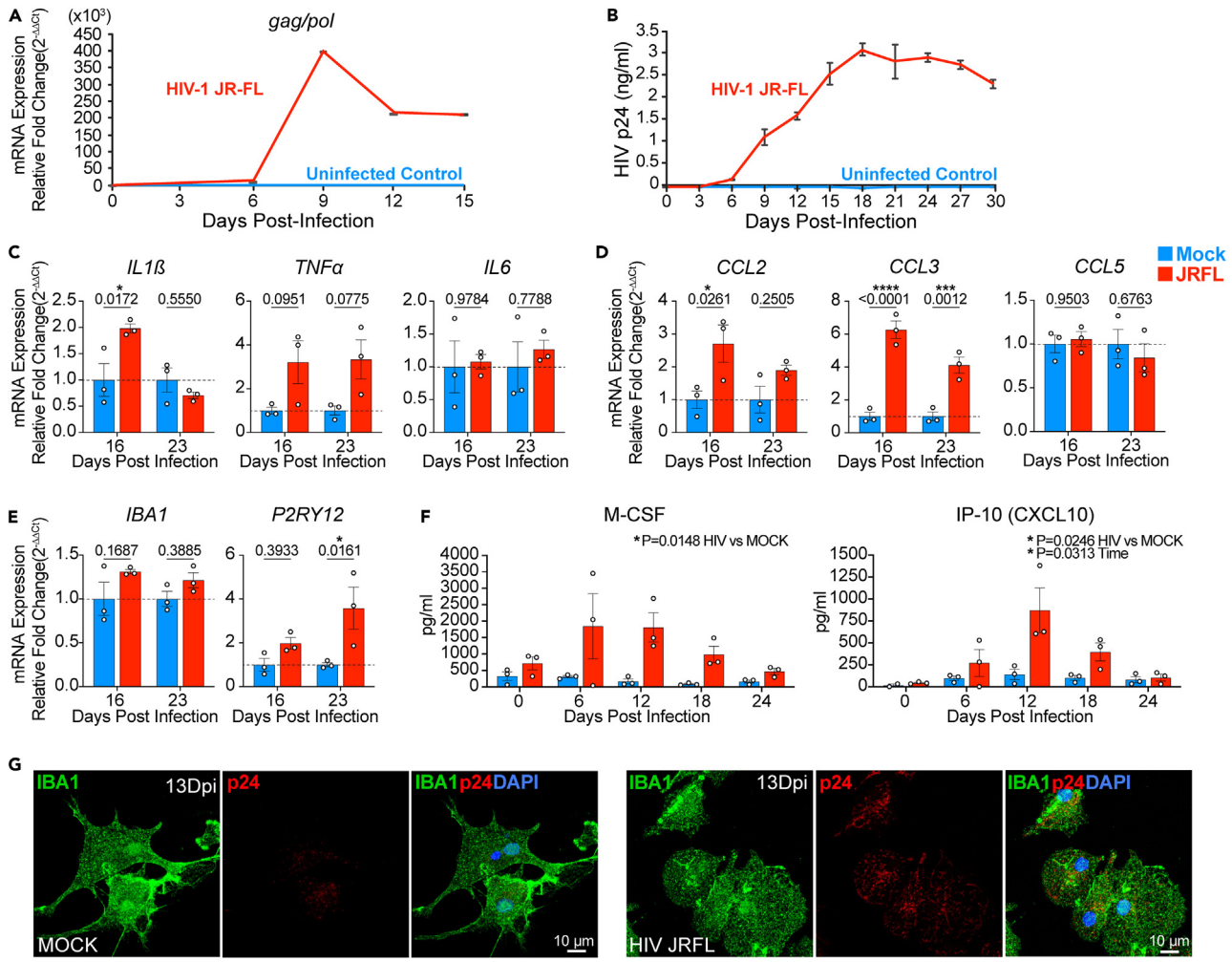

Figure 2. HIV-1-infected microglia exhibit productive infection, activation, and dysregulated cytokine/chemokine production

(A) RT-qPCR analysis of viral *gag/pol* mRNA after infection with HIV-1 JRFL in microglia monocultures; $n = 3$ independent infections of 03SF line iPSC-derived microglia; data are presented as the mean ± SEM.

(B) ELISA analysis of secreted p24 in the culture supernatant of microglia infected with HIV-1 JR-FL reveals productive infection; $n = 3$ independent infections of 03SF iPSC-derived microglia; data are presented as the mean ± SEM.

(C) RT-qPCR analysis of *IL1β*, *TNFα* and *IL-6* mRNA at days 16 and 23 post infection with HIV-1 JRFL; $n = 3$ independent infections of 03SF iPSC-derived microglia; two-way ANOVA; Šídák multiple comparisons test; $*p < 0.05$; data are presented as the mean ± SEM.

(D) RT-qPCR analysis of *CCL2*, *CCL3*, and *CCL5* mRNA at days 16 and 23 post infection with HIV-1 JRFL; $n = 3$ independent infections of 03SF iPSC-derived microglia; two-way ANOVA; Šídák multiple comparisons test; $*p < 0.05$, $**p < 0.01$, $***p < 0.001$, $****p < 0.0001$; data are presented as the mean ± SEM.

(E) RT-qPCR analysis of *IBA1* and *P2RY12* mRNA at days 16 and 23 post infection with HIV-1 JRFL; $n = 3$ independent infections of 03SF iPSC-derived microglia; two-way ANOVA; Šídák multiple comparisons test; $*p < 0.05$; data are presented as the mean ± SEM.

(F) Luminex cytokine/chemokine analysis of secreted M-CSF and IP-10/CXCL10 culture supernatant from HIV-1 JRFL-infected microglia; $n = 3$ independent infections of 03SF microglia, two-way ANOVA or Mixed-effects model, respectively; Šídák or Holm-Šídák multiple comparisons test, respectively; $*p < 0.05$; data are presented as the mean ± SEM.

(G) Representative confocal images of nucleocapsid protein p24 staining in HIV-1 JRFL-infected 03SF-derived microglia ($IBA1^+$). Scale bars, 10 µm.

After establishing the infectability of iPSC microglia with HIV-1 JRFL, we then asked whether HIV-1 infection elicits differential expression of inflammatory and canonical microglial mRNAs using reverse transcription-quantitative PCR (RT-qPCR). In this second experiment we found HIV-1 infection augmented the expression of the inflammation-associated genes interleukin 1β (*IL1β*, on day 16) and tumor necrosis factor alpha (*TNFα*), while the expression of interleukin 6 (*IL6*) displayed no change (Figure 2C). We then examined the mRNA expression of the chemokines *CCL2* (monocyte chemoattractant protein 1, *MCP-1*), *CCL3* (macrophage inflammatory protein 1 alpha, *MIP-1*), and *CCL5* (RANTES). These three chemokines play important roles in immune cell recruitment and migration to sites of inflammation and infection and have been found to be elevated in cognitively impaired individuals with HIV-1.[63] A significant elevation in the mRNA expression of

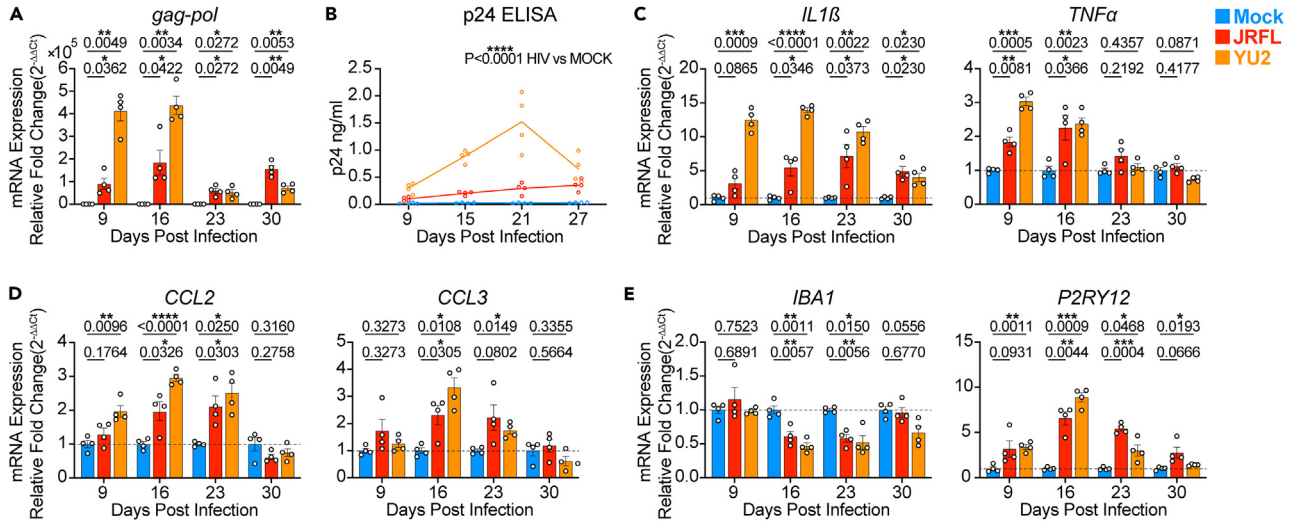

Figure 3. HIV-1-infected microglia exhibit productive infection, activation, and dysregulated cytokine/chemokine production

(A) RT-qPCR analysis of viral *gag/pol* mRNA at days 9, 16, 23, and 30 post infection with HIV-1 JRFL and HIV-1 YU2; two-way ANOVA; $*p < 0.05$, $**p < 0.01$; $n = 3$ independent infections of CD06 iPSC-derived microglia; data are presented as the mean ± SEM.

(B) ELISA analysis of secreted p24 in the culture supernatant of microglia infected with HIV-1 JRFL and HIV-1 YU2 at days 9, 15, 21, and 27 reveals productive infection; $n = 3$ independent infections of CD06 iPSC-derived microglia; two-way ANOVA; $****p < 0.0001$; data are presented as the mean ± SEM.

(C) RT-qPCR analysis of *IL1β* and *TNFα* mRNA at days 9, 16, 23, and 30 post infection with HIV-1 JRFL and HIV-1 YU2; $n = 3$ independent infections of CD06 iPSC-derived microglia; two-way ANOVA; Holm-Šídák multiple comparisons test; $*p < 0.05$, $**p < 0.01$, $***p < 0.001$, $****p < 0.0001$; data are presented as the mean ± SEM.

(D) RT-qPCR analysis of *CCL2* and *CCL3* mRNA at days 9, 16, 23, and 30 post infection with HIV-1 JRFL and HIV-1 YU2; $n = 3$ independent infections of CD06 iPSC-derived microglia; two-way ANOVA; Holm-Šídák multiple comparisons test; $*p < 0.05$, $**p < 0.01$, $***p < 0.001$, $****p < 0.0001$; data are presented as the mean ± SEM.

(E) RT-qPCR analysis of *IBA1* and *P2RY12* mRNA at days 9, 16, 23, and 30 post infection with HIV-1 JRFL and HIV-1 YU2; $n = 3$ independent infections of CD06 iPSC-derived microglia; two-way ANOVA; Holm-Šídák multiple comparisons test; $*p < 0.05$, $**p < 0.01$, $***p < 0.001$; data are presented as the mean ± SEM.

CCL2 and *CCL3* was observed by day 16 post infection, whereas the expression of *CCL5* remained unchanged (Figure 2D). To assess whether microglial identity was altered by HIV-1 infection, we assessed the mRNA expression of the canonical microglial genes *IBA1* and *P2RY12*. While IBA1 remained stable, *P2RY12* exhibited significantly increased expression by day 23 post infection (Figure 2E). Next, we asked how HIV-1 infection might alter microglial chemokine and cytokine production. Although the levels of most cytokines were below the detection threshold (Table S3), we noted a significant surge in the secretion of chemokines M-CSF and interferon inducible protein 10 (IP-10/CXCL10) following HIV-1 infection in the same supernatant used in Figure 2B (Figure 2F). Finally, to visualize HIV-1 infected cells, we detected HIV-1 p24 protein using a biotin-streptavidin amplification protocol.[64] On day 13 post infection with JRFL, p24 positive microglia were found (Figure 2G). Collectively, our findings suggest that iPSC-derived microglia can sustain an R5 tropic HIV-1 infection and exhibit an inflammatory activation profile consistent with previous studies.

To confirm that HIV-1 JRFL infection of human iPSC-derived microglia resulted in productive infection and inflammatory activation, we chose a female iPSC line, CD06, and infected it with the JRFL strain as well as a second R5 tropic HIV-1 strain, YU2,[65] isolated from the CSF of a different patient with severe HAND. We confirmed infection by RT-qPCR of viral *gag-pol* RNA, which exhibited significantly increased expression for both strains by day 16 post infection, with a subsequent decrease (Figure 3A). Using ELISA to detect secreted p24 revealed productive infection for both viral strains (Figure 3B). We then assessed the expression of key inflammatory markers and microglial core mRNAs by qPCR. Both JRFL and YU2 infections led to a significant increase in *IL1β* expression compared to uninfected microglia (Figure 3C). Similarly, *TNFα* was significantly upregulated in the first two weeks of infection but decreased as the productive infection waned (Figure 3C). We also observed increased expression of the chemokines *CCL2* and *CCL3* by days 16 and 23 post infection with both strains (Figure 3D). This upregulation then decreased by day 27, correlating with the reduction of productive infection as indicated by the p24 ELISA (Figure 3A). In comparison to the unaltered IBA1 expression we found previously, HIV-1 led to a significant reduction in IBA1 expression in CD06-infected microglia (Figure 3E). Similar to 03SF-infected microglia, CD06 had significant increased expression of *P2RY12* (Figure 3E). Together, these results demonstrate infectability of human iPSC-derived microglia with multiple, macrophage tropic HIV-1 strains and their ability to elicit an inflammatory response.

Type I interferon stimulated gene expression and sustained activation following HIV-1 infection

To investigate the transcriptional landscape of HIV-1-infected microglia, we performed bulk RNA sequencing on male 03SF iPSC-derived microglia infected by HIV-1 JRFL day 16 post infection. Principal component analysis (PCA) revealed clear separation of the infected vs. mock infected

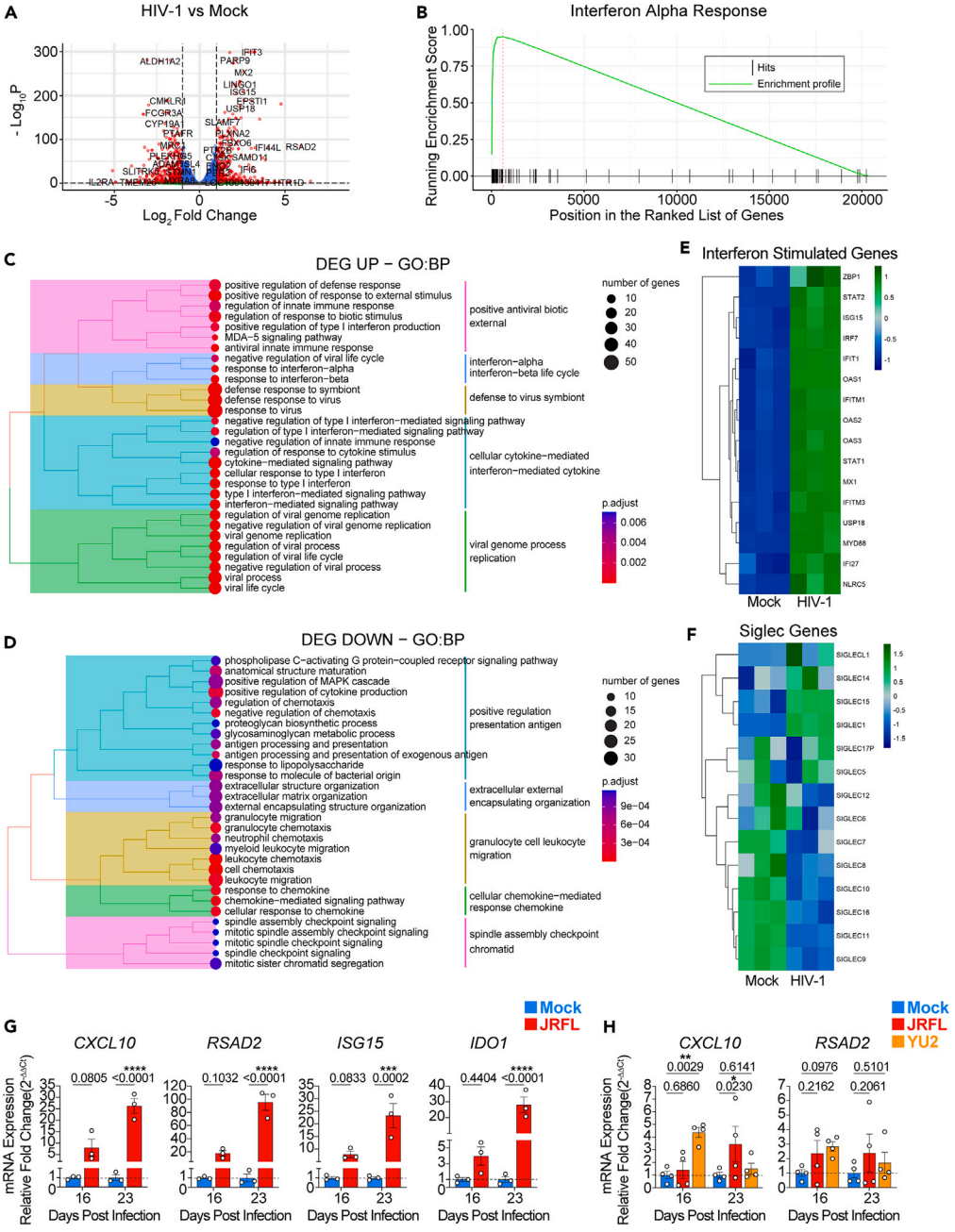

Figure 4. HIV-1 causes enrichment of type I interferon signaling pathways and sustained interferon activation

(A) A volcano plot illustrating differentially expressed genes (DEGs) in HIV-1 JRFL-infected vs. mock-infected microglia on day 16 post infection; *n* = 3 independent infections of 03SF line iPSC-derived microglia.

(B) GSEA plot showing enrichment of IFNα-responsive genes in HIV-1 JRFL-infected vs. mock-infected microglia on day 16 post infection (NES, normalized enrichment score; FDR, false discovery rate).

(C) Gene Ontology (GO) analysis of upregulated DEGs in HIV-1 JRFL vs. mock-infected microglia on day 16 post infection; *n* = 3 independent infections of 03SF microglia.

(D) Gene Ontology (GO) analysis of downregulated DEGs in HIV-1 JRFL vs. mock-infected microglia on day 16 post infection; *n* = 3 independent infections of 03SF microglia.

(E) A heatmap illustrating significant upregulation of interferon-stimulated genes in HIV-1-infected vs. mock-infected microglia on day 16 post infection; *n* = 3 independent infections of 03SF microglia.

Figure 4. *Continued*

(F) A heatmap illustrating *SIGLEC* gene expression in HIV-1-infected vs. mock-infected microglia on day 16 post infection; $n = 3$ independent infections of 03SF microglia.

(G) RT-qPCR analysis of *CXCL10*, *RSAD2*, *ISG15*, and *IDO1* mRNA from HIV-1 JRFL-infected vs. mock-infected microglia at days 16 and 23 post infection; $n = 3$ independent infections of 03SF iPSC-derived microglia, two-way ANOVA; uncorrected Fisher's LSD; $^{***}p < 0.001$, $^{****}p < 0.0001$; data are presented as the mean ± SEM.

(H) RT-qPCR analysis of *CXCL10* and *RSAD2* mRNA from HIV-1 JRFL- and HIV-1 YU2-infected and mock-infected microglia at days 16 and 23 post infection; $n = 4$ independent infections of CD06 iPSC-derived microglia, two-way ANOVA; uncorrected Fisher's LSD; $^{*}p < 0.05$, $^{**}p < 0.01$; data are presented as the mean ± SEM.

samples (Figure S2). Differential gene analysis revealed differentially expressed genes (DEGs) including several classic ISGs, such as *IFIT3*, *MX2*, *ISG15*, *RSAD2*, and others (Figure 4A) (Table S4). Gene set enrichment analysis (GSEA) confirmed a significant enrichment of genes related to the interferon alpha response (Figure 4B) (Table S5). Gene ontology analysis identified activation of innate immune responses and several related terms in the biological process component (Figures 4C, 4D, and S3) (Table S6). The upregulated DEG GO set includes pathways falling into the overall signaling clusters related to interferon signaling and positive regulation of antiviral biotic, interferon alpha/beta, defense against virus, cytokine-mediated and interferon-mediated pathways, and negative regulation of viral processes. Among the downregulated DEG GO clusters are pathways related to positive regulation of antigen processing, extracellular organization, granulocyte/leukocyte migration, chemokine-mediated signaling, and spindle assembly checkpoints. Importantly, HIV-1 infection was found to lead to significant induction of many ISGs, including *ISG15*, *IRF7*, *MX1*, *OAS1*, *OAS2*, *OAS3*, *STAT1*, *CXCL10*, and *IFITM3* (Figures 4A and 4E). Figure 4F shows the expression of various genes encoding SIGLEC proteins that are responsible for regulating microglial cell-cell interactions (reviewed by Crocker et al.[66]). Consistent with previous studies, we found that HIV-1 infection causes significant upregulation of *SIGLEC1*, which has been implicated in the direct cell-cell transmission of HIV.[67,68] However, we found that *SIGLEC11* and *SIGLEC16* were significantly downregulated after infection.

We then validated the expression of a subset of the ISGs identified in the sequencing dataset by RT-qPCR of JRFL infected 03SF iPSC-derived microglia. We found significant upregulation of *CXCL10*, *RSAD2*, *ISG15*, and *IDO1* (Figure 4G). Elevated expression of these genes persisted over an additional week of infection on day 23 (Figure 4G). Additionally, we performed RT-qPCR on CD06 iPSC-derived microglia infected with either JRFL or YU2 HIV strains. We also found increased expression of *CXCL10* and *RSAD2* in these HIV-infected cells; however, only the day 16 YU2 condition reached significance (Figure 4H). Comparison of Figures 4G and 4H indicates potential differences with infecting different cell lines. Together, these data support the conclusion that HIV-1 infection induces sustained type I interferon signaling in iPSC-derived microglia and alters the gene regulation of many microglial biological processes including interferon signaling.

HIV-1-infected microglia incorporate into cerebral organoids

After characterizing the response of isolated human iPSC-derived microglia to HIV-1 infection we then investigated whether HIV-1-infected microglia could incorporate into iPSC-derived cerebral organoids and whether interferon signaling was similarly upregulated in microglia and potentially other neural cell types. Cerebral organoids were grown using modified, published protocols.[47,69–73] To create microglia-containing organoids, we cocultured human microglia with sliced neocortical organoids (SNO), prepared as described previously.[73] SNOs exhibit enhanced neurogenesis and laminar expansion.[73] We found that microglia exhibit the ability to incorporate with organoid slices to form human microglia containing sliced neocortical organoids (mSNOs). Figure 5A shows mSNO containing neurons ($MAP2^+$), astrocytes ($GFAP^+$), and microglia ($IBA1^+$). These neuroimmune organoids provide a model system for studying the impact of HIV-1 infection on the physiology, localization, and interactions of these three cell types.

To create an HIV-1-infected human cerebral organoid, we infected 03SF iPSC-derived microglia with JRFL HIV. Following 2 weeks in culture, infected or noninfected microglia were added to 400 μM organoid slices and cultured for 2 additional weeks. On day 14 post coculture with microglia, mSNOs were fixed for immunohistochemistry or total RNA was extracted for RT-qPCR analysis. HIV-1-infected microglia ($p24^+$, $IBA1^+$) were detected in a mSNO (Figures 5B and 5C). Interestingly, neurons ($MAP2^+$) appeared to be sparser in regions of HIV-1-infected microglia (Figure 5B "arrows"). These regions had scattered $MAP2^+$ processes (Figure 5B1) compared with the denser MAP2 staining throughout the bulk of the organoid. HIV-1 *gag/pol* RNA exhibited significant expression in mSNOs containing HIV-1-infected microglia (Figure 5D). To provide evidence of productive infection in mSNOs, we identified secreted p24 only in the medium of organoid cultures that had received HIV-1-infected microglia (Figure 5E).

Because we observed significant and sustained interferon signaling in microglial monocultures, we evaluated mRNA expression of a panel of ISGs (*ISG15*, *RSAD2*, *IFITM3*, *MX1*, *IFI44*, and *IFI27*). We found that *ISG15* mRNA was significantly upregulated and *RSAD2* also showed an increasing trend of expression in mSNOs containing HIV-1-infected microglia (Figure 5F). *IFITM3* has been touted as a marker for interferon-responsive microglia and has been shown to play a newly discovered role in amyloid precursor protein processing to amyloid beta.[74] Interestingly, we found significant upregulation of *IFITM3* mRNA in mSNOs containing HIV-1-infected microglia (Figure 5F). We also evaluated the expression of *MX1*, *IFI27*, and *IFI44*, which, along with *ISG15* and *RSAD2*, were among the top 10 persistently upregulated genes in a recent study on two cohorts of 22 HIV-1 seroconverts from Uganda and 22 from South Africa.[75] Expression of *MX1*, *IFI27*, and *IFI44* appeared to be increased but failed to reach significance. Especially considering the small fraction of HIV-1-infected microglia in the cultured mSNO (Figure 5B), these increases suggest that HIV-1-infected microglia are associated with increased interferon signaling in the organoids and may have indirect consequences for neuronal viability and inflammatory responses in other cell types.

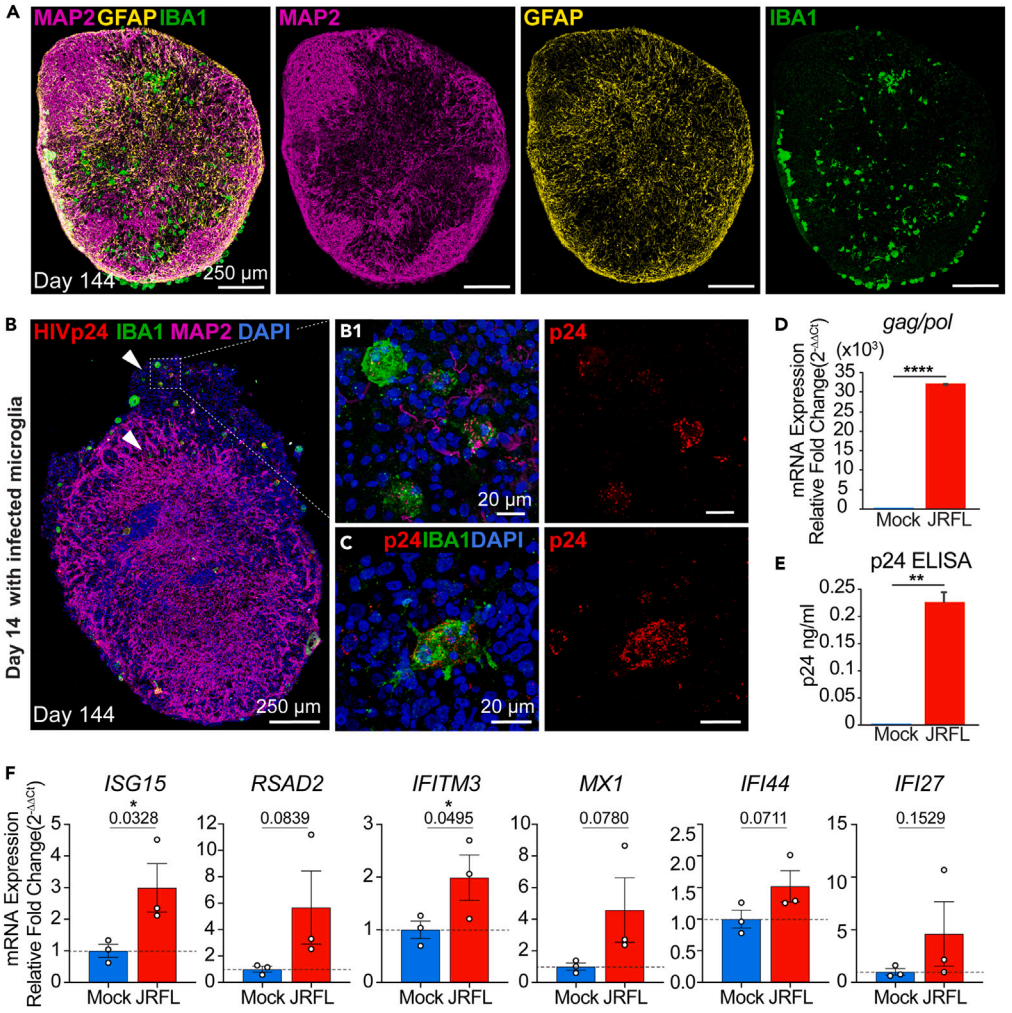

Figure 5. HIV-1-infected microglia incorporate into sliced cerebral organoids

(A) Representative confocal images of a day 144 organoid with neurons (MAP2$^+$), astrocytes (GFAP$^+$), and microglia (IBA1$^+$). Scale bars, 250 μm.

(B) Representative confocal images of day 144 organoids 14 days after the addition of HIV-1 JRFL-infected or mock-infected microglia; (B1) shows a high-magnification image of HIV-1-infected microglia from (B). Scale bars, 250 μm or 20 μm as indicated.

(C) High-magnification image of a single HIV-1-infected microglial cell within a sliced organoid. Scale bars, 20 μm.

(D) RT-qPCR of *gag/pol* mRNA from HIV-1 JRFL-infected or mock-infected microglia organoids on day 14; $n = 3$ independent infections of 03SF microglia; one-tailed t test; ****$p < 0.0001$; data are presented as the mean ± SEM.

(E) ELISA analysis of secreted p24 in culture supernatant from HIV-1 JRFL-infected or mock-infected microglia organoid day 14; $n = 3$ independent infections of 03SF microglia; one-tailed t test; **$p < 0.01$; data are presented as the mean ± SEM.

(F) RT-qPCR analysis of *ISG15*, *RSAD2*, *IFITM3*, *MX1*, *IFI44*, and *IFI27* mRNA from HIV-1 JRFL-infected or mock-infected microglia organoids on day 14; $n = 3$ independent infections of 03SF microglia; one-tailed t test; *$p < 0.05$; data are presented as the mean ± SEM.

DISCUSSION

In this study, we used iPSC-derived human microglia and microglia containing cortical organoids to model HIV-1 related neuroimmune dysregulation and pathology. In this model, iPSC-derived microglia (both male and female) were shown to be infected with two strains of replication competent HIV-1, JRFL and YU2, and exhibited inflammatory activation, as shown by gene expression changes and cytokine/chemokine secretion (Figures 2 and 3). Importantly, we found persistent activation of type I interferon response pathways and downstream interferon stimulated genes (ISGs), which may have important implications for understanding the pathogenesis of HAND.

In comparison to the recently developed primary human neural progenitor cell-derived organoid HIV-1 model[51] and the 2D neuron, astrocyte, and microglia "triculture" HIV-1 model,[50] an iPSC-derived human microglia containing sliced neocortical organoid model has distinct advantages. Organoids recapitulate 3D cell-cell and cell-matrix interactions more faithfully than 2D cultures and develop complex tissue architecture[70,76–79]; thus, organoids are well suited to studying aspects of altered brain anatomy and physiology seen in individuals with *HAND*.[6,80,81] While others have also generated microglia containing organoids using a protocol in which microglia innately develop within

organoids, this system is associated with a high degree of heterogeneous cell types,[52] which could make dissection of the relative contributions and effects on specific cell types more complex. In our method, we have greater freedom to manipulate the timing, proportion, and infection stage of microglia addition in sliced neocortical organoids. While some previous studies used pseudotyped virus,[51] our study examined infection using two macrophage tropic, replication competent strains of HIV-1. Our findings, showing induction of inflammatory gene expression associated with active viral expression align with recent studies on brain samples from HIV-1$^+$ patients from the National NeuroAIDS Tissue Consortium (NNTC). In that study, HIV-1 RNA load was found to correlate with increased interferon signaling and inflammatory gene sets while inversely correlating with neuronal and synaptic gene sets, suggesting neuronal pathology.[82]

Microglia secrete diverse cytokines and chemokines implicated in HIV-1 neuropathology.[83–85] Cytokine/chemokine analysis of the supernatant of HIV-1-infected microglia identified the secretion of M-CSF and IP-10/CXCL10 (Figure 2F). M-CSF overexpression has been linked to microglial proliferation, increased phagocytosis, cytokine secretion, and inflammatory responses in both AD and HAND, as well as increased microglial susceptibility to HIV-1 infection and increased virus replication.[86–91] IP-10/CXCL10 is a chemotactic chemokine that recruits leukocytes, T cells, and monocytes while also being neurotoxic and strongly correlated with HIV-1-related disease progression.[92–94] Clinical studies have shown elevated IP-10/CXCL10 levels (~200–1000 pg/mL) in the cerebral spinal fluid of people living with HIV-1[95,96]; these levels are strikingly similar to our observations (Figure 2F). CXCL10/IP-10 has been shown to be induced by HIV-1 proteins gp120, Nef, and Tat.[92,94,97,98] Importantly, IP-10/CXCL10 and RANTES (CCL5) were the strongest predictors of neurocognitive impairment in a screen of 139 people living with HIV-1,[99] similar to findings from earlier studies.[100,101] HIV-1 brain infection leads to an abnormal inflammatory state and dysregulated cytokine/chemokine production.[10,13,15] Despite this knowledge, there remains a large gap in our understanding of how CXCL10 and other cytokines/chemokines associated with CNS HIV-1 infection alter aspects of neuronal excitability, synaptic transmission, and inward and outward currents vital to healthy neuronal physiology.

A striking finding in our study was the persistent activation of interferon response genes over time in the microglial infection and also observed at two weeks after infection of the bulk iPSC-derived human microglia containing sliced neocortical organoid model. Induction of these pathways is known to be a hallmark of HIV-1 infection in monocytes and macrophages, much more prominently than in T cells.[102–105] Thus, it is not surprising to have seen this strong response in microglia, which share many physiologic properties with macrophages (reviewed by Li and Barres[106]). Most studies suggest that the interferon response is relatively transient; thus, the persistent expression in the microglial cell infection of at least a subset of ISGs may be a relatively unique feature of microglial HIV-1 infection that may have important pathophysiologic consequences. It will be of interest to determine the persistence and cellular sources of interferon-stimulated gene expression in the microglia containing sliced neocortical organoid model; however, even transient expression in this system may have important and possibly pathogenic consequences. Increasing evidence suggests a role for type I interferons in cognitive-related deficits seen in patients with various neurodegenerative diseases. Using single-cell sequencing, researchers have dissected a unique sub-population of interferon-responsive microglia that may potentiate dysregulated immune interactions in the form of aberrant pruning of synapses, altered phagocytic function, and dysregulated cytokine/chemokine production.[107] Constitutive overexpression of type I interferons seen in the "interferonopathies" can be associated with profound CNS disease (reviewed by Goldmann et al.[108] and Blank and Prinz[109]).[110] Patients receiving type I interferons therapeutically may experience cognitive impairment and neurological symptoms.[31–36]

Whether interferon induction inhibits or enhances HIV infection and latency in microglia remains to be understood. Recent studies have highlighted that interferon can inhibit HIV infection of primary microglia but less so of iPSC-derived microglia, as well as macrophages.[111,112] Interestingly, interferon may promote latency in macrophages.[113] An important feature of HIV infection of microglia identified in previous *in vitro* studies has been the rapid induction of viral latency.[14,114] Our cerebral organoid model will provide an interesting system to examine the induction of HIV latency, its reactivation, and its effects on both adjacent and more distant neural cells.

An important future direction, facilitated by the development of this model system, will be experiments aimed at understanding the functional consequences that HIV infection, dysregulated interferon signaling, inflammatory activity, and changes in other important genes expressed in the CNS, may have on neuronal synaptic transmission. Many ISGs have predicted downstream effects that could trigger or enhance neurodegeneration. For example, indoleamine 2,3-dioxygenase 1 (IDO) is a key enzyme in tryptophan catabolism, leading to the formation of kynurenic acid, an antagonist of NMDA receptors.[115] This pathway and its products, such as the neurotoxin and NMDAR antagonist quinolinic acid, have been previously implicated in neurodegenerative diseases, including Huntington's, Alzheimer's, and Parkinson's disease.[116,117] In addition to ISG's, Siglec genes, specifically *SIGLEC11* and *SIGLEC16*, are gaining interest as modulators of neuronal and glial interactions in the brain. Acting as immune checkpoints through their sialic acid binding, these two genes delicately balance activating and inhibitory inflammatory signaling pathways (reviewed by Linnartz-Gerlach et al[118] and Linnartz-Gerlach et al.[119]). Discovered in 2005 as a recent uniquely hominid gene, *SIGLEC16* arose from a gene-conversion event in *SIGLEC11*[120] altering the transmembrane and cytoplasmic tail domains to favor DAP12-associated activation pathways.[121] Intriguingly, *SIGLEC11* is exclusively expressed in the human brain and plays a neuroprotective role, particularly by preventing inappropriate microglial phagocytosis during inflammation.[122] The observed downregulation of these genes following HIV-1 infection suggests a potential increased vulnerability of neurons to microglial phagocytosis, highlighting a risk for exacerbated neuronal damage in HIV-associated neurocognitive disorders. Finally, while IBA1 expression was not affected by HIV-1 infection in our model, similar to a previous human HIV-1 organoid model,[51] purinergic receptor *P2RY12* displayed increased gene expression following HIV-1 infection (Figures 2E and 3E). P2Y12 is a G_i-coupled purinergic receptor allowing microglial chemotaxis to sites of injury by sensing extracellular ATP/ADP gradients.[123] Increased expression of *P2RY12* following HIV-1 infection in microglia may increase microglial motility, migration, and sensitivity to extracellular ATP.

Overall, the HIV-1 mSNO model presents an effective *in vitro* platform for investigating the underlying molecular and cellular mechanisms associated with HIV-1 and human neural cell interactions. Our results predict that interferon stimulated genes likely play a role in altering neuronal function and contributing to HAND.

Limitations of the study

Here, we report on the consequences of HIV-1 infection on human iPSC-derived microglia, finding dysregulated IFN signaling and inflammatory activation. We do not yet understand the functional effects these responses have on neuronal cell viability and synaptic transmission, and how these relate to the clinical manifestations of HAND. Furthermore, while our organoids facilitate study of neuroimmune interactions between neurons, astrocytes, and microglia, the model does not include peripheral immune cells known to play important roles in host defense and immunomodulation of the CNS (reviewed by Yang et al.[124]). Future studies could incorporate these other cell types to examine CNS cellular crosstalk with peripheral immune cells.

HIV-1 exhibits high genetic variability[112] in the global population and disease manifestations are clearly affected by patient comorbidities and genetic background (reviewed by Santoro and Perno,[125] McLaren and Fellay,[126] and Saylor et al.[127]). For example, it is clear that not every HIV-infected individual develops HAND. Our use of cells derived from three patient backgrounds and of two HIV-1 strains is therefore a limitation of the current study. Future studies would benefit from incorporating more HIV-1 strains and more importantly, larger sample sizes of iPSC-derived microglia, derived from multiple genetic backgrounds to truly characterize the pathology and investigate the underlying mechanisms.

HAND is a chronic disease that can take decades to develop (reviewed by Saylor et al.[127] and Clifford and Ances[128]), while our *in vitro* experiments explored HIV-1 infection over a matter of two to four weeks. Despite the effects that we observed, it must be noted that this study may not fully capture long-term consequences of *in vivo* infection, such as chronic inflammation, synaptic dysfunction, cellular senescence, and degeneration. However, because organoids can be cultured potentially for up to a year or more,[129] our model could be used to explore extended infection that might reflect neurological sequelae over time. It is important to note that cerebral organoids show a resemblance to prenatal neural tissue based on single cell RNA sequencing.[130,131] Therefore, the limited maturation of cell types within organoids may not fully represent what occurs in mature, *in vivo* tissue, such as would be expected in the brain of aging HIV-infected adults, much more commonly prevalent now in the era of highly effective anti-retroviral therapy. Despite these limitations, cerebral organoids offer significant potential for modeling aspects of HAND and HIV-1 dysregulation of neuroimmune interactions, and our studies serve as a basis for the development of future work to more fully elucidate important pathogenic mechanisms.

STAR★METHODS

Detailed methods are provided in the online version of this paper and include the following:

- KEY RESOURCES TABLE
- RESOURCE AVAILABILITY
  - Lead contact
  - Materials availability
  - Data and code availability
- EXPERIMENTAL MODEL AND STUDY PARTICIPANT DETAILS
  - Human iPSC lines
- METHOD DETAILS
  - Human induced pluripotent stem cell maintenance
  - Generation of microglia
  - Generation of iPSC-derived cerebral organoids
  - Organoid slicing
  - HIV-1 stock preparation
  - HIV-1 infection
  - HIV-1 2-LTR circles PCR
  - Tissue preparation
  - Immunofluorescence
  - RNA isolation
  - RT–qPCR
  - Bulk RNA sequencing and analysis
- QUANTIFICATION AND STATISTICAL ANALYSIS

SUPPLEMENTAL INFORMATION

Supplemental information can be found online at https://doi.org/10.1016/j.isci.2024.109628.

ACKNOWLEDGMENTS

This work was supported in part by grants from the NIH (R21NS120806 and R01AA023797), a Rutgers Busch Biomedical Grant, a Rutgers Brain Health Institute Pilot Grant, and support to the Child Health Institute of New Jersey from the Robert Wood Johnson Foundation (grant #74260). AJB was supported by NIH NIGMS T32GM8339 and NIH NCATS TL1TR003019.

AUTHOR CONTRIBUTIONS

A.J.B., Z.P.P., P.J., R.P.H., and A.B.R. conceived the study. A.J.B. designed the experiments and interpreted the data. A.J.B. performed most of the experiments with technical assistance from A.C.S., H.-C.L., and Y.A. A.C.S. and A.J.B. performed qPCR. H.-C.L. and A.J.B. performed ELISA. A.J.B. performed immunocytochemistry, immunohistochemistry, and confocal imaging. A.J.B., A.C.S., and H.-C.L. performed viral cultures. R.P.H. and A.J.B. performed computational analysis of RNA sequencing data. A.J.B. prepared the figures and wrote the manuscript with input from all coauthors.

DECLARATION OF INTERESTS

The authors declare no competing interests.

Received: October 31, 2023
Revised: February 1, 2024
Accepted: March 26, 2024
Published: March 28, 2024

REFERENCES

1. Simioni, S., Cavassini, M., Annoni, J.M., Rimbault Abraham, A., Bourquin, I., Schiffer, V., Calmy, A., Chave, J.P., Giacobini, E., Hirschel, B., and Du Pasquier, R.A. (2010). Cognitive dysfunction in HIV patients despite long-standing suppression of viremia. AIDS *24*, 1243–1250. https://doi.org/10.1097/QAD.0b013e3283354a7b.
2. Sacktor, N., Skolasky, R.L., Seaberg, E., Munro, C., Becker, J.T., Martin, E., Ragin, A., Levine, A., and Miller, E. (2016). Prevalence of HIV-associated neurocognitive disorders in the Multicenter AIDS Cohort Study. Neurology *86*, 334–340. https://doi.org/10.1212/wnl.0000000000002277.
3. Eggers, C., Arendt, G., Hahn, K., Husstedt, I.W., Maschke, M., Neuen-Jacob, E., Obermann, M., Rosenkranz, T., Schielke, E., and Straube, E.; German Association of Neuro-AIDS und Neuro-Infectiology DGNANI (2017). HIV-1-associated neurocognitive disorder: epidemiology, pathogenesis, diagnosis, and treatment. J. Neurol. *264*, 1715–1727. https://doi.org/10.1007/s00415-017-8503-2.
4. Sacktor, N. (2018). Changing clinical phenotypes of HIV-associated neurocognitive disorders. J. Neurovirol. *24*, 141–145. https://doi.org/10.1007/s13365-017-0556-6.
5. Lew, B.J., McDermott, T.J., Wiesman, A.I., O'Neill, J., Mills, M.S., Robertson, K.R., Fox, H.S., Swindells, S., and Wilson, T.W. (2018). Neural dynamics of selective attention deficits in HIV-associated neurocognitive disorder. Neurology *91*, e1860. https://doi.org/10.1212/WNL.0000000000006504.
6. Israel, S.M., Hassanzadeh-Behbahani, S., Turkeltaub, P.E., Moore, D.J., Ellis, R.J., and Jiang, X. (2019). Different roles of frontal versus striatal atrophy in HIV-associated neurocognitive disorders. Hum. Brain Mapp. *40*, 3010–3026. https://doi.org/10.1002/hbm.24577.
7. Koenig, S., Gendelman, H.E., Orenstein, J.M., Dal Canto, M.C., Pezeshkpour, G.H., Yungbluth, M., Janotta, F., Aksamit, A., Martin, M.A., and Fauci, A.S. (1986). Detection of AIDS virus in macrophages in brain tissue from AIDS patients with encephalopathy. Science *233*, 1089–1093. https://doi.org/10.1126/science.3016903.
8. Gendelman, H.E., Lipton, S.A., Tardieu, M., Bukrinsky, M.I., and Nottet, H.S. (1994). The neuropathogenesis of HIV-1 infection. J. Leukoc. Biol. *56*, 389–398. https://doi.org/10.1002/jlb.56.3.389.
9. Rappaport, J., Joseph, J., Croul, S., Alexander, G., Del Valle, L., Amini, S., and Khalili, K. (1999). Molecular pathway involved in HIV-1-induced CNS pathology: role of viral regulatory protein. J. Leukoc. Biol. *65*, 458–465. https://doi.org/10.1002/jlb.65.4.458.
10. González-Scarano, F., and Martín-García, J. (2005). The neuropathogenesis of AIDS. Nat. Rev. Immunol. *5*, 69–81. https://doi.org/10.1038/nri1527.
11. Kraft-Terry, S.D., Buch, S.J., Fox, H.S., and Gendelman, H.E. (2009). A Coat of Many Colors: Neuroimmune Crosstalk in Human Immunodeficiency Virus Infection. Neuron *64*, 133–145. https://doi.org/10.1016/j.neuron.2009.09.042.
12. Lindl, K.A., Marks, D.R., Kolson, D.L., and Jordan-Sciutto, K.L. (2010). HIV-Associated Neurocognitive Disorder: Pathogenesis and Therapeutic Opportunities. J. Neuroimmune Pharmacol. *5*, 294–309. https://doi.org/10.1007/s11481-010-9205-z.
13. Burdo, T.H., Lackner, A., and Williams, K.C. (2013). Monocyte/macrophages and their role in HIV neuropathogenesis. Immunol. Rev. *254*, 102–113.
14. Alvarez-Carbonell, D., Ye, F., Ramanath, N., Garcia-Mesa, Y., Knapp, P.E., Hauser, K.F., and Karn, J. (2019). Cross-talk between microglia and neurons regulates HIV latency. PLoS Pathog. *15*, e1008249. https://doi.org/10.1371/journal.ppat.1008249.
15. Kaul, M., Garden, G.A., and Lipton, S.A. (2001). Pathways to neuronal injury and apoptosis in HIV-associated dementia. Nature *410*, 988–994. https://doi.org/10.1038/35073667.
16. Kaul, M., Zheng, J., Okamoto, S., Gendelman, H.E., and Lipton, S.A. (2005). HIV-1 infection and AIDS: consequences for the central nervous system. Cell Death Differ. *12*, 878–892. https://doi.org/10.1038/sj.cdd.4401623.
17. Hofer, M.J., and Campbell, I.L. (2013). Type I interferon in neurological disease—The devil from within. Cytokine Growth Factor Rev. *24*, 257–267. https://doi.org/10.1016/j.cytogfr.2013.03.006.
18. McGlasson, S., Jury, A., Jackson, A., and Hunt, D. (2015). Type I interferon dysregulation and neurological disease. Nat. Rev. Neurol. *11*, 515–523. https://doi.org/10.1038/nrneurol.2015.143.
19. Platanias, L.C. (2005). Mechanisms of type-I- and type-II-interferon-mediated signalling. Nat. Rev. Immunol. *5*, 375–386. https://doi.org/10.1038/nri1604.
20. Roy, E.R., Wang, B., Wan, Y.-W., Chiu, G., Cole, A., Yin, Z., Propson, N.E., Xu, Y., Jankowsky, J.L., Liu, Z., et al. (2020). Type I interferon response drives neuroinflammation and synapse loss in Alzheimer disease. J. Clin. Invest. *130*, 1912–1930. https://doi.org/10.1172/JCI133737.
21. Roy, E.R., Chiu, G., Li, S., Propson, N.E., Kanchi, R., Wang, B., Coarfa, C., Zheng, H., and Cao, W. (2022). Concerted type I interferon signaling in microglia and neural cells promotes memory impairment associated with amyloid β plaques. Immunity *55*, 879–894.e876. https://doi.org/10.1016/j.immuni.2022.03.018.
22. Lee, J.S., and Shin, E.-C. (2020). The type I interferon response in COVID-19: implications for treatment. Nat. Rev. Immunol. *20*, 585–586. https://doi.org/10.1038/s41577-020-00429-3.
23. Phetsouphanh, C., Darley, D.R., Wilson, D.B., Howe, A., Munier, C.M.L., Patel, S.K., Juno, J.A., Burrell, L.M., Kent, S.J., Dore, G.J., et al. (2022). Immunological

dysfunction persists for 8 months following initial mild-to-moderate SARS-CoV-2 infection. Nat. Immunol. *23*, 210–216. https://doi.org/10.1038/s41590-021-01113-x.

24. Baruch, K., Deczkowska, A., David, E., Castellano, J.M., Miller, O., Kertser, A., Berkutzki, T., Barnett-Itzhaki, Z., Bezalel, D., Wyss-Coray, T., et al. (2014). Aging-induced type I interferon response at the choroid plexus negatively affects brain function. Science *346*, 89–93. https://doi.org/10.1126/science.1252945.
25. Rho, M.B., Wesselingh, S., Glass, J.D., McArthur, J.C., Choi, S., Griffin, J., and Tyor, W.R. (1995). A Potential Role for Interferon-α in the Pathogenesis of HIV-Associated Dementia. Brain Behav. Immun. *9*, 366–377. https://doi.org/10.1006/brbi.1995.1034.
26. Krivine, A., Force, G., Servan, J., Cabée, A., Rozenberg, F., Dighiero, L., Marguet, F., and Lebon, P. (1999). Measuring HIV-1 RNA and interferon-alpha in the cerebrospinal fluid of AIDS patients: insights into the pathogenesis of AIDS Dementia Complex. J. Neurovirol. *5*, 500–506. https://doi.org/10.3109/13550289909045379.
27. Perrella, O., Carreiri, P.B., Perrella, A., Sbreglia, C., Gorga, F., Guarnaccia, D., and Tarantino, G. (2001). Transforming growth factor beta-1 and interferon-alpha in the AIDS dementia complex (ADC): possible relationship with cerebral viral load? Eur. Cytokine Netw. *12*, 51–55.
28. Anderson, A.M., Lennox, J.L., Mulligan, M.M., Loring, D.W., Zetterberg, H., Blennow, K., Kessing, C., Koneru, R., Easley, K., and Tyor, W.R. (2017). Cerebrospinal fluid interferon alpha levels correlate with neurocognitive impairment in ambulatory HIV-Infected individuals. J. Neurovirol. *23*, 106–112. https://doi.org/10.1007/s13365-016-0466-z.
29. Solomon, I.H., Chettimada, S., Misra, V., Lorenz, D.R., Gorelick, R.J., Gelman, B.B., Morgello, S., and Gabuzda, D. (2020). White Matter Abnormalities Linked to Interferon, Stress Response, and Energy Metabolism Gene Expression Changes in Older HIV-Positive Patients on Antiretroviral Therapy. Mol. Neurobiol. *57*, 1115–1130. https://doi.org/10.1007/s12035-019-01795-3.
30. Merimsky, O., Reider-Groswasser, I., Inbar, M., and Chaitchik, S. (1990). Interferon-related mental deterioration and behavioral changes in patients with renal cell carcinoma. Eur. J. Cancer *26*, 596–600. https://doi.org/10.1016/0277-5379(90)90086-9.
31. Christina, A.M., Randall, S.S., and Arthur, D.F. (1991). Persistent neurotoxicity of systemically administered interferon-alpha. Neurology *41*, 672. https://doi.org/10.1212/WNL.41.5.672.
32. Pavol, M.A., Meyers, C.A., Rexer, J.L., Valentine, A.D., Mattis, P.J., and Talpaz, M. (1995). Pattern of neurobehavioral deficits associated with interferon alfa therapy for leukemia. Neurology *45*, 947–950. https://doi.org/10.1212/wnl.45.5.947.
33. Capuron, L., Ravaud, A., and Dantzer, R. (2001). Timing and Specificity of the Cognitive Changes Induced by Interleukin-2 and Interferon-α Treatments in Cancer Patients. Psychosom. Med. *63*, 376–386.
34. Capuron, L., Gumnick, J.F., Musselman, D.L., Lawson, D.H., Reemsnyder, A., Nemeroff, C.B., and Miller, A.H. (2002). Neurobehavioral Effects of Interferon-α in Cancer Patients: Phenomenology and Paroxetine Responsiveness of Symptom Dimensions. Neuropsychopharmacology *26*, 643–652. https://doi.org/10.1016/S0893-133X(01)00407-9.
35. Wichers, M.C., Koek, G.H., Robaeys, G., Praamstra, A.J., and Maes, M. (2005). Early increase in vegetative symptoms predicts IFN-α-induced cognitive-depressive changes. Psychol. Med. *35*, 433–441. https://doi.org/10.1017/S0033291704003526.
36. Raison, C.L., Demetrashvili, M., Capuron, L., and Miller, A.H. (2005). Neuropsychiatric Adverse Effects of Interferon-α. CNS Drugs *19*, 105–123. https://doi.org/10.2165/00023210-200519020-00002.
37. Paolicelli, R.C., Bolasco, G., Pagani, F., Maggi, L., Scianni, M., Panzanelli, P., Giustetto, M., Ferreira, T.A., Guiducci, E., Dumas, L., et al. (2011). Synaptic Pruning by Microglia Is Necessary for Normal Brain Development. Science *333*, 1456–1458.
38. Casano, A.M., and Peri, F. (2015). Microglia: Multitasking Specialists of the Brain. Dev. Cell *32*, 469–477. https://doi.org/10.1016/j.devcel.2015.01.018.
39. Durafourt, B.A., Moore, C.S., Zammit, D.A., Johnson, T.A., Zaguia, F., Guiot, M.C., Bar-Or, A., and Antel, J.P. (2012). Comparison of polarization properties of human adult microglia and blood-derived macrophages. Glia *60*, 717–727. https://doi.org/10.1002/glia.22298.
40. Gosselin, D., Skola, D., Coufal, N.G., Holtman, I.R., Schlachetzki, J.C.M., Sajti, E., Jaeger, B.N., O'Connor, C., Fitzpatrick, C., Pasillas, M.P., et al. (2017). An environment-dependent transcriptional network specifies human microglia identity. Science *356*, eaal3222. https://doi.org/10.1126/science.aal3222.
41. Song, W.M., and Colonna, M. (2018). The identity and function of microglia in neurodegeneration. Nat. Immunol. *19*, 1048–1058. https://doi.org/10.1038/s41590-018-0212-1.
42. Hammond, T.R., Dufort, C., Dissing-Olesen, L., Giera, S., Young, A., Wysoker, A., Walker, A.J., Gergits, F., Segel, M., Nemesh, J., et al. (2019). Single-Cell RNA Sequencing of Microglia throughout the Mouse Lifespan and in the Injured Brain Reveals Complex Cell-State Changes. Immunity *50*, 253–271.e6. https://doi.org/10.1016/j.immuni.2018.11.004.
43. Byrnes, S.J., Angelovich, T.A., Busman-Sahay, K., Cochrane, C.R., Roche, M., Estes, J.D., and Churchill, M.J. (2022). Non-Human Primate Models of HIV Brain Infection and Cognitive Disorders. Viruses *14*, 1997. https://doi.org/10.3390/v14091997.
44. Moretti, S., Virtuoso, S., Sernicola, L., Farcomeni, S., Maggiorella, M.T., and Borsetti, A. (2021). Advances in SIV/SHIV Non-Human Primate Models of NeuroAIDS. Pathogens *10*, 1018. https://doi.org/10.3390/pathogens10081018.
45. Abud, E.M., Ramirez, R.N., Martinez, E.S., Healy, L.M., Nguyen, C.H.H., Newman, S.A., Yeromin, A.V., Scarfone, V.M., Marsh, S.E., Fimbres, C., et al. (2017). iPSC-Derived Human Microglia-like Cells to Study Neurological Diseases. Neuron *94*, 278–293.e9. https://doi.org/10.1016/j.neuron.2017.03.042.
46. Ormel, P.R., Vieira de Sá, R., van Bodegraven, E.J., Karst, H., Harschnitz, O., Sneeboer, M.A.M., Johansen, L.E., van Dijk, R.E., Scheefhals, N., Berdenis van Berlekom, A., et al. (2018). Microglia innately develop within cerebral organoids. Nat. Commun. *9*, 4167. https://doi.org/10.1038/s41467-018-06684-2.
47. Xu, R., Boreland, A.J., Li, X., Erickson, C., Jin, M., Atkins, C., Pang, Z.P., Daniels, B.P., and Jiang, P. (2021). Developing human pluripotent stem cell-based cerebral organoids with a controllable microglia ratio for modeling brain development and pathology. Stem Cell Rep. *16*, 1923–1937. https://doi.org/10.1016/j.stemcr.2021.06.011.
48. Vaughan-Jackson, A., Stodolak, S., Ebrahimi, K.H., Browne, C., Reardon, P.K., Pires, E., Gilbert-Jaramillo, J., Cowley, S.A., and James, W.S. (2021). Differentiation of human induced pluripotent stem cells to authentic macrophages using a defined, serum-free, open-source medium. Stem Cell Rep. *16*, 1735–1748. https://doi.org/10.1016/j.stemcr.2021.05.018.
49. Rai, M.A., Hammonds, J., Pujato, M., Mayhew, C., Roskin, K., and Spearman, P. (2020). Comparative analysis of human microglial models for studies of HIV replication and pathogenesis. Retrovirology *17*, 35. https://doi.org/10.1186/s12977-020-00544-y.
50. Ryan, S.K., Gonzalez, M.V., Garifallou, J.P., Bennett, F.C., Williams, K.S., Sotuyo, N.P., Mironets, E., Cook, K., Hakonarson, H., Anderson, S.A., and Jordan-Sciutto, K.L. (2020). Neuroinflammation and EIF2 Signaling Persist despite Antiretroviral Treatment in an hiPSC Tri-culture Model of HIV Infection. Stem Cell Rep. *14*, 703–716. https://doi.org/10.1016/j.stemcr.2020.02.010.
51. dos Reis, R.S., Sant, S., Keeney, H., Wagner, M.C.E., and Ayyavoo, V. (2020). Modeling HIV-1 neuropathogenesis using three-dimensional human brain organoids (hBORGs) with HIV-1 infected microglia. Sci. Rep. *10*, 15209. https://doi.org/10.1038/s41598-020-72214-0.
52. Gumbs, S.B.H., Berdenis van Berlekom, A., Kübler, R., Schipper, P.J., Gharu, L., Boks, M.P., Ormel, P.R., Wensing, A.M.J., de Witte, L.D., and Nijhuis, M. (2022). Characterization of HIV-1 Infection in Microglia-Containing Human Cerebral Organoids. Viruses *14*, 829. https://doi.org/10.3390/v14040829.
53. Min, A.K., Javidfar, B., Missall, R., Doanman, D., Durens, M., Vil, S.S., Masih, Z., Graziani, M., Mordelt, A., Marro, S., et al. (2023). HIV-1 infection of genetically engineered iPSC-derived central nervous system-engrafted microglia in a humanized mouse model. Preprint at bioRxiv *1*. https://doi.org/10.1101/2023.04.26.538461.
54. Haenseler, W., Sansom, S.N., Buchrieser, J., Newey, S.E., Moore, C.S., Nicholls, F.J., Chintawar, S., Schnell, C., Antel, J.P., Allen, N.D., et al. (2017). A Highly Efficient Human Pluripotent Stem Cell Microglia Model Displays a Neuronal-Co-culture-Specific Expression Profile and Inflammatory Response. Stem Cell Rep. *8*, 1727–1742. https://doi.org/10.1016/j.stemcr.2017.05.017.
55. Claes, C., Van den Daele, J., and Verfaillie, C.M. (2018). Generating tissue-resident macrophages from pluripotent stem cells: Lessons learned from microglia. Cell. Immunol. *330*, 60–67. https://doi.org/10.1016/j.cellimm.2018.01.019.

56. Vodyanik, M.A., Thomson, J.A., and Slukvin, I.I. (2006). Leukosialin (CD43) defines hematopoietic progenitors in human embryonic stem cell differentiation cultures. Blood *108*, 2095–2105. https://doi.org/10.1182/blood-2006-02-003327.
57. Koyanagi, Y., Miles, S., Mitsuyasu, R.T., Merrill, J.E., Vinters, H.V., and Chen, I.S. (1987). Dual infection of the central nervous system by AIDS viruses with distinct cellular tropisms. Science *236*, 819–822. https://doi.org/10.1126/science.3646751.
58. Merrill, J.E., Koyanagi, Y., Zack, J., Thomas, L., Martin, F., and Chen, I.S. (1992). Induction of interleukin-1 and tumor necrosis factor alpha in brain cultures by human immunodeficiency virus type 1. J. Virol. *66*, 2217–2225.
59. Yu, H., Rabson, A.B., Kaul, M., Ron, Y., and Dougherty, J.P. (1996). Inducible human immunodeficiency virus type 1 packaging cell lines. J. Virol. *70*, 4530–4537. https://doi.org/10.1128/jvi.70.7.4530-4537.1996.
60. Chargelegue, D., and O'Toole, C.M. (1992). Development of a sensitive ELISA for HIV-1 p24 antigen using a fluorogenic substrate for monitoring HIV-1 replication in vitro. J. Virol. Methods *38*, 323–332. https://doi.org/10.1016/0166-0934(92)90077-Q.
61. Marodon, G., Warren, D., Filomio, M.C., and Posnett, D.N. (1999). Productive infection of double-negative T cells with HIV in vivo. Proc. Natl. Acad. Sci. USA *96*, 11958–11963. https://doi.org/10.1073/pnas.96.21.11958.
62. Butler, S.L., Hansen, M.S., and Bushman, F.D. (2001). A quantitative assay for HIV DNA integration in vivo. Nat. Med. *7*, 631–634. https://doi.org/10.1038/87979.
63. Letendre, S.L., Lanier, E.R., and McCutchan, J.A. (1999). Cerebrospinal fluid beta chemokine concentrations in neurocognitively impaired individuals infected with human immunodeficiency virus type 1. J. Infect. Dis. *180*, 310–319. https://doi.org/10.1086/314866.
64. Eugenin, E.A., and Berman, J.W. (2016). Improved Methods to Detect Low Levels of HIV Using Antibody-Based Technologies. Methods Mol. Biol. *1354*, 265–279. https://doi.org/10.1007/978-1-4939-3046-3_18.
65. Li, Y., Kappes, J.C., Conway, J.A., Price, R.W., Shaw, G.M., and Hahn, B.H. (1991). Molecular characterization of human immunodeficiency virus type 1 cloned directly from uncultured human brain tissue: identification of replication-competent and -defective viral genomes. J. Virol. *65*, 3973–3985. https://doi.org/10.1128/jvi.65.8.3973-3985.1991.
66. Crocker, P.R., Paulson, J.C., and Varki, A. (2007). Siglecs and their roles in the immune system. Nat. Rev. Immunol. *7*, 255–266. https://doi.org/10.1038/nri2056.
67. Izquierdo-Useros, N., Lorizate, M., Puertas, M.C., Rodriguez-Plata, M.T., Zangger, N., Erikson, E., Pino, M., Erkizia, I., Glass, B., Clotet, B., et al. (2012). Siglec-1 Is a Novel Dendritic Cell Receptor That Mediates HIV-1 Trans-Infection Through Recognition of Viral Membrane Gangliosides. PLoS Biol. *10*, e1001448. https://doi.org/10.1371/journal.pbio.1001448.
68. Zou, Z., Chastain, A., Moir, S., Ford, J., Trandem, K., Martinelli, E., Cicala, C., Crocker, P., Arthos, J., and Sun, P.D. (2011). Siglecs Facilitate HIV-1 Infection of Macrophages through Adhesion with Viral Sialic Acids. PLoS One *6*, e24559. https://doi.org/10.1371/journal.pone.0024559.
69. Lancaster, M.A., and Knoblich, J.A. (2014). Generation of cerebral organoids from human pluripotent stem cells. Nat. Protoc. *9*, 2329–2340. https://doi.org/10.1038/nprot.2014.158.
70. Paşca, A.M., Sloan, S.A., Clarke, L.E., Tian, Y., Makinson, C.D., Huber, N., Kim, C.H., Park, J.-Y., O'Rourke, N.A., Nguyen, K.D., et al. (2015). Functional cortical neurons and astrocytes from human pluripotent stem cells in 3D culture. Nat. Methods *12*, 671–678. https://doi.org/10.1038/nmeth.3415.
71. Sloan, S.A., Andersen, J., Paşca, A.M., Birey, F., and Paşca, S.P. (2018). Generation and assembly of human brain region–specific three-dimensional cultures. Nat. Protoc. *13*, 2062–2085. https://doi.org/10.1038/s41596-018-0032-7.
72. Yoon, S.-J., Elahi, L.S., Paşca, A.M., Marton, R.M., Gordon, A., Revah, O., Miura, Y., Walczak, E.M., Holdgate, G.M., Fan, H.C., et al. (2019). Reliability of human cortical organoid generation. Nat. Methods *16*, 75–78. https://doi.org/10.1038/s41592-018-0255-0.
73. Qian, X., Su, Y., Adam, C.D., Deutschmann, A.U., Pather, S.R., Goldberg, E.M., Su, K., Li, S., Lu, L., Jacob, F., et al. (2020). Sliced Human Cortical Organoids for Modeling Distinct Cortical Layer Formation. Cell Stem Cell *26*, 766–781.e9. https://doi.org/10.1016/j.stem.2020.02.002.
74. Hur, J.Y., Frost, G.R., Wu, X., Crump, C., Pan, S.J., Wong, E., Barros, M., Li, T., Nie, P., Zhai, Y., et al. (2020). The innate immunity protein IFITM3 modulates γ-secretase in Alzheimer's disease. Nature *586*, 735–740. https://doi.org/10.1038/s41586-020-2681-2.
75. Mackelprang, R.D., Filali-Mouhim, A., Richardson, B., Lefebvre, F., Katabira, E., Ronald, A., Gray, G., Cohen, K.W., Klatt, N.R., Pecor, T., et al. (2023). Upregulation of IFN-stimulated genes persists beyond the transitory broad immunologic changes of acute HIV-1 infection. iScience *26*, 106454. https://doi.org/10.1016/j.isci.2023.106454.
76. Lancaster, M.A., Renner, M., Martin, C.-A., Wenzel, D., Bicknell, L.S., Hurles, M.E., Homfray, T., Penninger, J.M., Jackson, A.P., and Knoblich, J.A. (2013). Cerebral organoids model human brain development and microcephaly. Nature *501*, 373–379. https://doi.org/10.1038/nature12517.
77. Birey, F., Andersen, J., Makinson, C.D., Islam, S., Wei, W., Huber, N., Fan, H.C., Metzler, K.R.C., Panagiotakos, G., Thom, N., et al. (2017). Assembly of functionally integrated human forebrain spheroids. Nature *545*, 54–59. https://doi.org/10.1038/nature22330.
78. Quadrato, G., Nguyen, T., Macosko, E.Z., Sherwood, J.L., Min Yang, S., Berger, D.R., Maria, N., Scholvin, J., Goldman, M., Kinney, J.P., et al. (2017). Cell diversity and network dynamics in photosensitive human brain organoids. Nature *545*, 48–53. https://doi.org/10.1038/nature22047.
79. Velasco, S., Kedaigle, A.J., Simmons, S.K., Nash, A., Rocha, M., Quadrato, G., Paulsen, B., Nguyen, L., Adiconis, X., Regev, A., et al. (2019). Individual brain organoids reproducibly form cell diversity of the human cerebral cortex. Nature *570*, 523–527. https://doi.org/10.1038/s41586-019-1289-x.
80. Di Sclafani, V., Mackay, R.D., Meyerhoff, D.J., Norman, D., Weiner, M.W., and Fein, G. (1997). Brain atrophy in HIV infection is more strongly associated with CDC clinical stage than with cognitive impairment. J. Int. Neuropsychol. Soc. *3*, 276–287.
81. Clifford, K.M., Samboju, V., Cobigo, Y., Milanini, B., Marx, G.A., Hellmuth, J.M., Rosen, H.J., Kramer, J.H., Allen, I.E., and Valcour, V.G. (2017). Progressive Brain Atrophy Despite Persistent Viral Suppression in HIV Patients Older Than 60 Years. J. Acquir. Immune Defic. Syndr. *76*, 289–297. https://doi.org/10.1097/QAI.0000000000001489.
82. Sanna, P.P., Fu, Y., Masliah, E., Lefebvre, C., and Repunte-Canonigo, V. (2021). Central nervous system (CNS) transcriptomic correlates of human immunodeficiency virus (HIV) brain RNA load in HIV-infected individuals. Sci. Rep. *11*, 12176. https://doi.org/10.1038/s41598-021-88052-7.
83. Hanisch, U.K. (2002). Microglia as a source and target of cytokines. Glia *40*, 140–155. https://doi.org/10.1002/glia.10161.
84. Ramesh, G., MacLean, A.G., and Philipp, M.T. (2013). Cytokines and Chemokines at the Crossroads of Neuroinflammation, Neurodegeneration, and Neuropathic Pain. Mediators Inflamm. *2013*, 480739. https://doi.org/10.1155/2013/480739.
85. Chen, N.C., Partridge, A.T., Sell, C., Torres, C., and Martín-García, J. (2017). Fate of microglia during HIV-1 infection: From activation to senescence? Glia *65*, 431–446. https://doi.org/10.1002/glia.23081.
86. Gallo, P., Pagni, S., Giometto, B., Piccinno, M.G., Bozza, F., Argentiero, V., and Tavolato, B. (1990). Macrophage-colony stimulating factor (M-CSF) in the cerebrospinal fluid. J. Neuroimmunol. *29*, 105–112. https://doi.org/10.1016/0165-5728(90)90152-D.
87. Kalter, D.C., Nakamura, M., Turpin, J.A., Baca, L.M., Hoover, D.L., Dieffenbach, C., Ralph, P., Gendelman, H.E., and Meltzer, M.S. (1991). Enhanced HIV replication in macrophage colony-stimulating factor-treated monocytes. J. Immunol. *146*, 298–306.
88. Kutza, J., Crim, L., Feldman, S., Hayes, M.P., Gruber, M., Beeler, J., and Clouse, K.A. (2000). Macrophage Colony-Stimulating Factor Antagonists Inhibit Replication of HIV-1 in Human Macrophages. J. Immunol. *164*, 4955–4960. https://doi.org/10.4049/jimmunol.164.9.4955.
89. Mitrasinovic, O.M., Perez, G.V., Zhao, F., Lee, Y.L., Poon, C., and Murphy, G.M. (2001). Overexpression of Macrophage Colony-stimulating Factor Receptor on Microglial Cells Induces an Inflammatory Response. J. Biol. Chem. *276*, 30142–30149. https://doi.org/10.1074/jbc.M104265200.
90. Kutza, J., Fields, K., Grimm, T.A., and Clouse, K.A. (2002). Inhibition of HIV replication and macrophage colony-stimulating factor production in human macrophages by antiretroviral agents. AIDS Res. Hum. Retroviruses *18*, 619–625. https://doi.org/10.1089/088922202760019310.
91. Smith, A.M., Gibbons, H.M., Oldfield, R.L., Bergin, P.M., Mee, E.W., Curtis, M.A., Faull, R.L.M., and Dragunow, M. (2013). M-CSF increases proliferation and phagocytosis

while modulating receptor and transcription factor expression in adult human microglia. J. Neuroinflammation *10*, 85. https://doi.org/10.1186/1742-2094-10-85.

92. van Marle, G., Henry, S., Todoruk, T., Sullivan, A., Silva, C., Rourke, S.B., Holden, J., McArthur, J.C., Gill, M.J., and Power, C. (2004). Human immunodeficiency virus type 1 Nef protein mediates neural cell death: a neurotoxic role for IP-10. Virology *329*, 302–318. https://doi.org/10.1016/j.virol.2004.08.024.
93. Jiao, Y., Zhang, T., Wang, R., Zhang, H., Huang, X., Yin, J., Zhang, L., Xu, X., and Wu, H. (2012). Plasma IP-10 Is Associated with Rapid Disease Progression in Early HIV-1 Infection. Viral Immunol. *25*, 333–337. https://doi.org/10.1089/vim.2012.0011.
94. Lei, J., Yin, X., Shang, H., and Jiang, Y. (2019). IP-10 is highly involved in HIV infection. Cytokine *115*, 97–103. https://doi.org/10.1016/j.cyto.2018.11.018.
95. Kolb, S.A., Sporer, B., Lahrtz, F., Koedel, U., Pfister, H.-W., and Fontana, A. (1999). Identification of a T cell chemotactic factor in the cerebrospinal fluid of HIV-1-infected individuals as interferon-γ inducible protein 10. J. Neuroimmunol. *93*, 172–181. https://doi.org/10.1016/S0165-5728(98)00223-9.
96. Peluso, M.J., Valcour, V., Phanuphak, N., Ananworanich, J., Fletcher, J.L.K., Chalermchai, T., Krebs, S.J., Robb, M.L., Hellmuth, J., Gisslén, M., et al. (2017). Immediate initiation of cART is associated with lower levels of cerebrospinal fluid YKL-40, a marker of microglial activation, in HIV-1 infection. AIDS *31*, 247–252. https://doi.org/10.1097/QAD.0000000000001314.
97. Kutsch, O., Oh, J., Nath, A., and Benveniste, E.N. (2000). Induction of the chemokines interleukin-8 and IP-10 by human immunodeficiency virus type 1 tat in astrocytes. J. Virol. *74*, 9214–9221. https://doi.org/10.1128/jvi.74.19.9214-9221.2000.
98. Asensio, V.C., Maier, J., Milner, R., Boztug, K., Kincaid, C., Moulard, M., Phillipson, C., Lindsley, K., Krucker, T., Fox, H.S., and Campbell, I.L. (2001). Interferon-independent, human immunodeficiency virus type 1 gp120-mediated induction of CXCL10/IP-10 gene expression by astrocytes in vivo and in vitro. J. Virol. *75*, 7067–7077. https://doi.org/10.1128/JVI.75.15.7067-7077.2001.
99. Ruhanya, V., Jacobs, G.B., Naidoo, S., Paul, R.H., Joska, J.A., Seedat, S., Nyandoro, G., Engelbrecht, S., and Glashoff, R.H. (2021). Impact of Plasma IP-10/CXCL10 and RANTES/CCL5 Levels on Neurocognitive Function in HIV Treatment-Naive Patients. AIDS Res. Hum. Retroviruses *37*, 657–665. https://doi.org/10.1089/aid.2020.0203.
100. Valverde-Villegas, J.M., de Medeiros, R.M., Ellwanger, J.H., Santos, B.R., Melo, M.G.d., Almeida, S.E.d.M., and Chies, J.A.B. (2018). High CXCL10/IP-10 levels are a hallmark in the clinical evolution of the HIV infection. Infect. Genet. Evol. *57*, 51–58. https://doi.org/10.1016/j.meegid.2017.11.002.
101. Burlacu, R., Umlauf, A., Marcotte, T.D., Soontornniyomkij, B., Diaconu, C.C., Bulacu-Talnariu, A., Temereanca, A., Ruta, S.M., Letendre, S., Ene, L., and Achim, C.L. (2020). Plasma CXCL10 correlates with HAND in HIV-infected women. J. Neurovirol. *26*, 23–31. https://doi.org/10.1007/s13365-019-00785-4.
102. Berg, R.K., Rahbek, S.H., Kofod-Olsen, E., Holm, C.K., Melchjorsen, J., Jensen, D.G., Hansen, A.L., Jørgensen, L.B., Ostergaard, L., Tolstrup, M., et al. (2014). T cells detect intracellular DNA but fail to induce type I IFN responses: implications for restriction of HIV replication. PLoS One *9*, e84513. https://doi.org/10.1371/journal.pone.0084513.
103. Aso, H., Ito, J., Koyanagi, Y., and Sato, K. (2019). Comparative Description of the Expression Profile of Interferon-Stimulated Genes in Multiple Cell Lineages Targeted by HIV-1 Infection. Front. Microbiol. *10*, 429. https://doi.org/10.3389/fmicb.2019.00429.
104. Elsner, C., Ponnurangam, A., Kazmierski, J., Zillinger, T., Jansen, J., Todt, D., Döhner, K., Xu, S., Ducroux, A., Kriedemann, N., et al. (2020). Absence of cGAS-mediated type I IFN responses in HIV-1-infected T cells. Proc. Natl. Acad. Sci. USA *117*, 19475–19486. https://doi.org/10.1073/pnas.2002481117.
105. Jeremiah, N., Ferran, H., Antoniadou, K., De Azevedo, K., Nikolic, J., Maurin, M., Benaroch, P., and Manel, N. (2023). RELA tunes innate-like interferon I/III responses in human T cells. J. Exp. Med. *220*, e20220666. https://doi.org/10.1084/jem.20220666.
106. Li, Q., and Barres, B.A. (2018). Microglia and macrophages in brain homeostasis and disease. Nat. Rev. Immunol. *18*, 225–242. https://doi.org/10.1038/nri.2017.125.
107. Jin, M., Xu, R., Wang, L., Alam, M.M., Ma, Z., Zhu, S., Martini, A.C., Jadali, A., Bernabucci, M., Xie, P., et al. (2022). Type-I-interferon signaling drives microglial dysfunction and senescence in human iPSC models of Down syndrome and Alzheimer's disease. Cell Stem Cell *29*, 1135–1153.e8. https://doi.org/10.1016/j.stem.2022.06.007.
108. Goldmann, T., Blank, T., and Prinz, M. (2016). Fine-tuning of type I IFN-signaling in microglia–implications for homeostasis, CNS autoimmunity and interferonopathies. Curr. Opin. Neurobiol. *36*, 38–42. https://doi.org/10.1016/j.conb.2015.09.003.
109. Blank, T., and Prinz, M. (2017). Type I interferon pathway in CNS homeostasis and neurological disorders. Glia *65*, 1397–1406. https://doi.org/10.1002/glia.23154.
110. Wiley, C.A., Steinman, R.A., and Wang, Q. (2023). Innate immune activation without immune cell infiltration in brains of murine models of Aicardi-Goutières Syndrome. Brain Pathol. *33*, e13118. https://doi.org/10.1111/bpa.13118.
111. Nasr, N., Alshehri, A.A., Wright, T.K., Shahid, M., Heiner, B.M., Harman, A.N., Botting, R.A., Helbig, K.J., Beard, M.R., Suzuki, K., et al. (2017). Mechanism of Interferon-Stimulated Gene Induction in HIV-1-Infected Macrophages. J. Virol. *91*, e00744-17. https://doi.org/10.1128/jvi.00744-17.
112. Woodburn, B.M., Kanchi, K., Zhou, S., Colaianni, N., Joseph, S.B., and Swanstrom, R. (2022). Characterization of Macrophage-Tropic HIV-1 Infection of Central Nervous System Cells and the Influence of Inflammation. J. Virol. *96*, e0095722. https://doi.org/10.1128/jvi.00957-22.
113. Dickey, L.L., Martins, L.J., Planelles, V., and Hanley, T.M. (2022). HIV-1-induced type I IFNs promote viral latency in macrophages. J. Leukoc. Biol. *112*, 1343–1356. https://doi.org/10.1002/jlb.4ma0422-616r.
114. Sreeram, S., Ye, F., Garcia-Mesa, Y., Nguyen, K., El Sayed, A., Leskov, K., and Karn, J. (2022). The potential role of HIV-1 latency in promoting neuroinflammation and HIV-1-associated neurocognitive disorder. Trends Immunol. *43*, 630–639. https://doi.org/10.1016/j.it.2022.06.003.
115. Schwarcz, R., and Stone, T.W. (2017). The kynurenine pathway and the brain: Challenges, controversies and promises. Neuropharmacology *112*, 237–247. https://doi.org/10.1016/j.neuropharm.2016.08.003.
116. Malpass, K. (2011). Neurodegenerative disease: the kynurenine pathway–promising new targets and therapies for neurodegenerative disease. Nat. Rev. Neurol. *7*, 417. https://doi.org/10.1038/nrneurol.2011.102.
117. Maddison, D.C., and Giorgini, F. (2015). The kynurenine pathway and neurodegenerative disease. Semin. Cell Dev. Biol. *40*, 134–141. https://doi.org/10.1016/j.semcdb.2015.03.002.
118. Linnartz-Gerlach, B., Kopatz, J., and Neumann, H. (2014). Siglec functions of microglia. Glycobiology *24*, 794–799. https://doi.org/10.1093/glycob/cwu044.
119. Linnartz-Gerlach, B., Mathews, M., and Neumann, H. (2014). Sensing the neuronal glycocalyx by glial sialic acid binding immunoglobulin-like lectins. Neuroscience *275*, 113–124. https://doi.org/10.1016/j.neuroscience.2014.05.061.
120. Hayakawa, T., Angata, T., Lewis, A.L., Mikkelsen, T.S., Varki, N.M., and Varki, A. (2005). A Human-Specific Gene in Microglia. Science *309*, 1693. https://doi.org/10.1126/science.1114321.
121. Cao, H., Lakner, U., de Bono, B., Traherne, J.A., Trowsdale, J., and Barrow, A.D. (2008). SIGLEC16 encodes a DAP12-associated receptor expressed in macrophages that evolved from its inhibitory counterpart SIGLEC11 and has functional and non-functional alleles in humans. Eur. J. Immunol. *38*, 2303–2315. https://doi.org/10.1002/eji.200738078.
122. Yiner, W., and Harald, N. (2010). Alleviation of Neurotoxicity by Microglial Human Siglec-11. J. Neurosci. *30*, 3482. https://doi.org/10.1523/JNEUROSCI.3940-09.2010.
123. Haynes, S.E., Hollopeter, G., Yang, G., Kurpius, D., Dailey, M.E., Gan, W.-B., and Julius, D. (2006). The P2Y12 receptor regulates microglial activation by extracellular nucleotides. Nat. Neurosci. *9*, 1512–1519. https://doi.org/10.1038/nn1805.
124. Yang, Q., Wang, G., and Zhang, F. (2020). Role of Peripheral Immune Cells-Mediated Inflammation on the Process of Neurodegenerative Diseases. Front. Immunol. *11*, 582825. https://doi.org/10.3389/fimmu.2020.582825.
125. Santoro, M.M., and Perno, C.F. (2013). HIV-1 Genetic Variability and Clinical Implications. ISRN Microbiol. *2013*, 481314. https://doi.org/10.1155/2013/481314.
126. McLaren, P.J., and Fellay, J. (2021). HIV-1 and human genetic variation. Nat. Rev. Genet. *22*, 645–657. https://doi.org/10.1038/s41576-021-00378-0.
127. Saylor, D., Dickens, A.M., Sacktor, N., Haughey, N., Slusher, B., Pletnikov, M., Mankowski, J.L., Brown, A., Volsky, D.J., and McArthur, J.C. (2016). HIV-associated neurocognitive disorder–pathogenesis and prospects for treatment. Nat. Rev. Neurol. *12*, 234–248. https://doi.org/10.1038/nrneurol.2016.27.
128. Clifford, D.B., and Ances, B.M. (2013). HIV-associated neurocognitive disorder. Lancet Infect. Dis. *13*, 976–986. https://doi.org/10.1016/s1473-3099(13)70269-x.

129. Sloan, S.A., Darmanis, S., Huber, N., Khan, T.A., Birey, F., Caneda, C., Reimer, R., Quake, S.R., Barres, B.A., and Paşca, S.P. (2017). Human Astrocyte Maturation Captured in 3D Cerebral Cortical Spheroids Derived from Pluripotent Stem Cells. Neuron *95*, 779–790.e6. https://doi.org/10.1016/j.neuron.2017.07.035.

130. Cheroni, C., Trattaro, S., Caporale, N., López-Tobón, A., Tenderini, E., Sebastiani, S., Troglio, F., Gabriele, M., Bressan, R.B., Pollard, S.M., et al. (2022). Benchmarking brain organoid recapitulation of fetal corticogenesis. Transl. Psychiatry *12*, 520. https://doi.org/10.1038/s41398-022-02279-0.

131. Camp, J.G., Badsha, F., Florio, M., Kanton, S., Gerber, T., Wilsch-Bräuninger, M., Lewitus, E., Sykes, A., Hevers, W., Lancaster, M., et al. (2015). Human cerebral organoids recapitulate gene expression programs of fetal neocortex development. Proc. Natl. Acad. Sci. USA *112*, 15672–15677. https://doi.org/10.1073/pnas.1520760112.

STAR★METHODS

KEY RESOURCES TABLE

REAGENT or RESOURCE	SOURCE	IDENTIFIER
Antibodies		
Mouse anti-CD43	Invitrogen	Cat# 14043982; RRID: AB_763493
Rabbit anti-CD235	Invitrogen	Cat# PA527154; RRID: AB_2544630
Mouse anti-IBA1	Sigma	Cat# SAB2702364; RRID: AB_2820253
Rabbit anti-IBA1	Wako Fujifilm	Cat# 01919741; RRID: AB_839504
Rabbit anti-P2Y12	Atlas Antibodies	Cat# HPA014518; RRID: AB_2669027
Rabbit anti-CX3CR1	BIO-RAD	Cat# AHP1589; RRID: AB_2087421
Mouse anti-TMEM119	Cell Signaling	Cat# 41134; RRID: AB_3073710
Rabbit anti-PU1	Cell Signaling	Cat# 2266; RRID: AB_10692379
Mouse anti-MAP2	Sigma	Cat# M1406; RRID: AB_477171
Chicken anti-MAP2	Millipore	Cat# AB5543; RRID: AB_571049
Rabbit anti-SYNAPSIN I(E028)	T.C. Sudhof, Stanford University	Cat# E028; RRID: AB_2315400
Rabbit anti-HIV1p24-Biotin	GeneTex	Cat# GTX64130; RRID: N/A
Rabbit anti-GFAP	DAKO	Cat# Z0334; RRID: AB_10013382
Goat anti-Mouse Alexa Fluor 488	Invitrogen	Cat# A11029; RRID: AB_2534088
Goat anti-Mouse Alexa Fluor 546	Invitrogen	Cat# A11030; RRID: AB_2534089
Goat anti-Mouse Alexa Fluor 633	Invitrogen	Cat# A21052; RRID: AB_2535719
Goat anti-Rabbit Alexa Fluor 488	Invitrogen	Cat# A11034; RRID: AB_2576217
Goat anti-Rabbit Alexa Fluor 546	Invitrogen	Cat# A11035; RRID: AB_2534093
Goat anti-Rabbit Alexa Fluor 633	Invitrogen	Cat# A21071; RRID: AB_141419
Goat Anti-Chicken Alexa Fluor 546	Invitrogen	Cat# A11040; RRID: AB_1500590
Steptavidin Alexa Fluor 546	Invitrogen	Cat# S11225; RRID: AB_2532130
Bacterial and virus strains		
HIV-1 JRFL	NIH HIV Reagent Program	Cat# ARP-395
HIV-1 YU2	NIH HIV Reagent Program	Cat# ARP-1350
Chemicals, peptides, and recombinant proteins		
BMP4	Peprotech	Cat# 120-05
VEGF 121	Peprotech	Cat# 100-21
SCF	Peprotech	Cat# 300-07
IL-3	Peprotech	Cat# 200-34
M-CSF	Peprotech	Cat# 300-25
IL-34	Peprotech	Cat# 200-34
GM-CSF	Peprotech	Cat# 500-P33
SB431542	Stemgent	Cat# 04-0010-05
DMEF12	HyClone	Cat# Sh3002201
N2	Gibco	Cat# 17502048
B27-RA	Gibco	Cat# 12587010
B27	Gibco	Cat# 17504044
Y-27632	Tocris	Cat# 125410
Growth factor-reduced Matrigel	Corning	Cat# 354230
BDNF	Peprotech	Cat# 450-02
GDNF	Peprotech	Cat# 450-10

(*Continued on next page*)

Continued

REAGENT or RESOURCE	SOURCE	IDENTIFIER
NT-3	Peprotech	Cat# 450-03
dibutyryl-cyclic AMP	Stemcell Technologies	Cat# 73882
L-Ascorbic Acid	Sigma	Cat# A4403
Critical commercial assays		
PowerUp SYBR Green Master Mix for qPCR	Applied Biosystems	Cat# A25776
RNAeasy Plus Mini Kit	Qiagen	Cat# 74134
HIV-1 Gag p24 DuoSet ELISA	R&D Systems	Cat# DY7360-05
Deposited data		
RNA sequencing data	This paper	NCBI GEO: GSE246082
Experimental models: Cell lines		
Cell lines	N/A	See Table S1 for detailed information
Oligonucleotides		
qPCR Primers	IDT	See Table S2 for detailed information
Software and algorithms		
Adobe Illustrator	Adobe	https://www.adobe.com/products/illustrator.html
Fiji	ImageJ	https://imagej.net/Fiji/Downloads
GraphPad Prism 10	GraphPad Software	N/A
R 4.1.0		https://www.r-project.org
RStudio	RStudio	https://www.rstudio.com/products/rstudio/download/
ZEN 2.3	Carl Zeiss	N/A

RESOURCE AVAILABILITY

Lead contact

Any additional information and requests for resources and reagents should be directed to and will be fulfilled by the lead contact, Arnold Rabson (rabsonab@rwjms.rutgers.edu).

Materials availability

This study did not generate new unique reagents.

Data and code availability

- The RNA sequencing datasets generated in this study have been deposited at NCBI GEO and are publicly available as of the date of publication. Accession numbers are listed in the key resources table.
- This paper does not report original code.
- Any additional information required to reanalyze the data reported in this work is available from the lead contact upon request.

EXPERIMENTAL MODEL AND STUDY PARTICIPANT DETAILS

Human iPSC lines

A total of three hiPSC lines, two males and one female, were used in this study (Table S1).

METHOD DETAILS

Human induced pluripotent stem cell maintenance

Three human iPSC lines were used in this study (male 03SF iPSC line; female CD06 iPSC line; male CD52 iPSC line) (Table S1). Human iPSCs were cultured in stem cell medium consisting of MACs iPS-Brew XF complete medium. The culture medium was changed daily. Human iPSCs were passaged one to two times per week onto new plates coated with Matrigel. Human iPSCs were detached with Accutase treatment for

5 min and centrifuged at 120 rcf for 5 min. The pellet was resuspended in stem cell medium plus Y-27632 (10 μM). The iPSCs used in this study were below passage 50. All studies were performed with protocols approved by Rutgers University.

Generation of microglia

Primitive microglia precursors (PMPs) were generated from 3 iPSC cell lines using a previously established protocol.[54] iPSCs were detached with Accutase, plated at 20,000 cells per well in a 96-well low-adherence plate in yolk sac induction medium plus the Rho kinase (ROCK) inhibitor Y-27632 (10 μM), and centrifuged at 1000 rpm for 3 min to aggregate the cells for embryoid body formation. Yolk-sac induction medium consisted of MAC iPS-Brew XF complete medium plus bone morphogenetic protein 4 (BMP4, 50 ng/mL), vascular endothelial growth factor (VEGF, 50 ng/mL), stem cell factor (SCF, 20 ng/mL), and β-mercaptoethanol. Yolk-sac induction medium was given for the first 5 days of culture. On day 6, yolk sac-embryoid bodies (YS-EBs) were plated in 100 mm cell culture plates in factory medium consisting of XVIVO15 supplemented with 0.5% NEAA, β-mercaptoethanol, macrophage colony stimulating factor (M-CSF, 100 ng/mL) and interleukin-3 (25 ng/mL). At 2–4 weeks after plating, human PMPs egress from the yolk sac lumen into the surrounding medium and are continuously produced for more than 3 months.

To mature PMPs into microglia, PMPs were transitioned to maturation medium composed of XVIVO15 supplemented with N2, Glutamax, 0.5% NEAA, interleukin-34 (IL-34, 100 ng/mL), granulocyte macrophage colony stimulating factor (GM-CSF, 10 ng/mL, and M-CSF (25 ng/mL) for 1–2 weeks. The medium was changed every 4 days. Cells were then detached with 20 min Accutase treatment and used for experiments.

Generation of iPSC-derived cerebral organoids

Cerebral organoids were generated from the 03SF iPSC line using adapted previously published protocols.[73] In this study, 9,000 iPSCs were cultured in low-adherence 96-well plates to form uniform embryoid bodies. On day 1, the medium was changed to neural induction medium composed of DMEM/F12 supplemented with 1X N2, 2 μM A83-01, and 2 μM dorsomorphin. On days 5 and 6, half of the medium was replaced with DMEM/F12 supplemented with 1X N2, 10 μM SB431542, and 1 μM CHIR99021. On day 7, EBs were embedded in a Growth-Factor-Reduced Matrigel 'cookie' as previously described.[73] Half of the medium was changed every two days until day 14. On day 14, organoids were dissociated from the Matrigel cookie and placed in low-adherence 6-well plates on an orbital shaker at 85 rpm. On day 16, organoids were fed 1:1 DMEF12: Neurobasal, 1X N2, 1X B27-RA, 0.5% NEAA, and 200 μM L-AA. Medium was replenished every 2–3 days until day 30. On day 30, the medium was changed to 1:1 DMEF12: Neurobasal, 1X N2, 1X B27, 0.5% NEAA, 200 μM L-AA, and 0.25% GFR-Matrigel. Half of the medium was changed every 3–4 days.

Organoid slicing

To create sliced neocortical organoid cultures, cerebral organoids were sectioned with a vibratome and transferred back into *in vitro* cell culture. Organoids were maintained for greater than 120 days before slicing for co-culture experiments. Briefly, a fresh stock of 3% low-melting temperature agarose in PBS was prepared and kept at 39°C to remain liquid. Artificial cerebral spinal fluid (ACSF) for sectioning contained (in mM): NaCl 125, KCl 2.5, $NaH_2PO_4 \cdot H_2O$ 1.25, $NaHCO_3$ 25, $MgCl_2$ 1.2, $CaCl_2$ 2.5, glucose ($C_6H_{12}O_6$) 2.5, and sucrose ($C_{12}H_{22}O_{11}$) 22.5. The ACSF was then bubbled with 5% CO_2/95% O_2 for 10 min before bivalent cations (in mM): $MgCl_2$ 1.2, $CaCl_2$ 0.625. The solution was then filtered through a 0.2-micron PES filter and returned to bubbling on ice. Cerebral organoids were then transferred to 37°C DMEF12, 200 μM L-AA, and 55 μM β-mercaptoethanol before being embedded in 3% low-melting temperature agarose. The agarose block containing organoids was then sectioned at 400 μM thickness. Slices were then subjected to two washing processes in Primocin-treated medium to reduce the chance of contamination. To create an HIV-1 infected human cerebral organoid, 03SF iPSC-derived microglia were infected with JRFL HIV. Following 2 weeks in culture, infected or noninfected microglia were added to 400 μM organoid slices and cultured for 2 additional weeks. On day 14 post coculture with microglia, mSNOs were fixed for immunohistochemistry or total RNA was extracted.

HIV-1 stock preparation

HIV-1 JRFL virus (ARP-395) and HIV-1 YU2 proviral DNA (ARP-1350) were obtained through the NIH HIV Reagent Program, Division of AIDS, NIAID. HIV-1 JRFL was propagated in phytohemagglutinin (PHA, 5 μg/mL)-stimulated human peripheral blood mononuclear cells. Viruses were harvested on days 7–10 post infection. HIV-1 YU2 stocks were generated by transfection of 293T cells with HIV-1 YU2 proviral DNA. The transfected cells were cocultivated with PHA-PBMCs 48 h after transfection, and cell supernatants were harvested 7 days after coculture. The YU2 HIV stocks were further propagated in PHA-PBMCs as described. The amount of viral p24 was determined using the HIV-1 Gag p24 DuoSet ELISA (R &D System, DY7360-05).

HIV-1 infection

PMPs were matured for 1–2 weeks in microglia maturation medium. Matured PMPs were then incubated with 2 ng/mL p24 of either JRFL strain or YU2 strain HIV-1 (NIH AIDS Repository) for 24 h at 300,000 cells per 100 μL of medium. After 24 h, DMEF12 was added, and the cells were centrifuged for 3 min at 120 rcf. The cells were then resuspended in microglia maturation medium minus M-CSF and plated. Half of the medium was changed every 3–6 days. To choose post-infection day timepoints for experiments, ELISA against P24 protein secreted into the medium of active cultures was analyzed to ensure that infection had taken place and was productive. Based on the ELISA data, which we consistently found began to peak just after two weeks of infection, appropriate post-infection days were chosen for various experiments.

HIV-1 2-LTR circles PCR

For detection of HIV 2-LTR circles, total DNA (including small nongenomic DNA) was isolated with a DNeasy Blood and Tissue kit (Qiagen 69504). Endpoint PCR analysis (Taq 2X Master Mix, NEB) was performed using 300 ng DNA template and 2-LTR circle primers: forward, MH535: 5′-AACTAGGGAACCCACTGCTTAAG-3′; reverse, MH536: 5′-TCCACAGATCAAGGATATCTTGTC-3′.[62]

Tissue preparation

Organoids were fixed in 4% PFA overnight at 4°C. Organoids were then transferred to 15% sucrose and 0.05% sodium azide in PBS for 24 h, followed by another 24 h in 30% sucrose and 0.05% sodium azide in PBS. Organoids were then embedded in OCT freezing medium and snap frozen on an ethanol dry ice slurry. Frozen embedded organoids were given at least 3 h to warm to −20°C before cryosectioning on a Leica cryostat at thicknesses between 10 and 30 μM. Sections were mounted on charged microscope slides (VWR) and placed on a slide warmer at 37°C for 30 min. Slides were then stored in a slide box at −20°C until used for staining.

Immunofluorescence

For immunocytochemistry, half of the medium was left in each well with an equal amount of 4% PFA and then added at a final concentration of 2% PFA overnight at 4°C. The next day, PFA was removed, and the cells were washed with PBS plus 0.3 M glycine for 30 min. The cells were then permeabilized with 0.2% Triton X-100 in PBS for 7 min. The cells were then blocked for 1 h in blocking buffer consisting of 5% normal goat serum (NGS), 4% bovine serum albumin (BSA), 0.05% Triton X-100, 0.05% sodium azide, and PBS.

For immunohistochemistry, cryosectioned organoid slides were warmed to 37°C for 5 min. A hydrophobic barrier was then drawn around the specimens and allowed to dry for 5 min. PBS plus 0.3 M glycine was then added in a liquid dome over the specimens to rehydrate for 10 min. Sections were permeabilized with 0.5% Triton X-100, 0.3 M glycine, and PBS for 1 h. After permeabilization, the sections were blocked with blocking solution consisting of 5% normal goat serum, 4% BSA, 0.05% Triton X-100, 0.05% sodium azide, and PBS for 1 h. Primary antibodies were diluted in blocking solution and applied to the sections overnight at 4°C. The primary antibodies are summarized in the key resources table. After washing with 0.05% Triton X-100 and PBS (PBST) 5 times, secondary antibodies diluted in blocking buffer were added for 1 h at RT. Finally, the sections were washed five times with PBST before a final wash in deionized water and mounting with DAPI Fluoroshield (Fisher). Secondary antibodies were Alexa Fluor 488-, 546-, 633- or 647-conjugated goat antibodies (Invitrogen) used at a 1:500 dilution. Images were taken on a Zeiss LSM700 confocal microscope.

RNA isolation

Total RNA was prepared with a RNeasy Plus kit (Qiagen) with preprocessing through Qiashredder (Qiagen) and frozen at −80°C.

RT–qPCR

cDNA was generated using SuperScript VILO Master mix. RNA expression was measured using SYBR green on a QuantStudio 3 (Agilent). Probes were generated using NCBI primer blast and are listed in Table S2. Two technical replicates were performed per sample. When a high standard deviation between replicates occurred, replicates were rerun in triplicate. All expression levels were normalized to GAPDH expression and represented as $2^{\wedge-(\Delta\Delta CT)}$. For null result values where a ct was not achieved, a max ct value of 40 was used for statistical analysis.

Bulk RNA sequencing and analysis

We performed bulk RNA sequencing analysis of iPSC-derived microglia. Total RNA was prepared using a RNeasy kit (QIAGEN). Library construction and sequencing were performed by Novogene. The libraries were subjected to 75 bp paired read sequencing using a NextSeq500 Illumina sequencer. Approximately 30–36 million paired reads were generated for each sample. Bc12Fastq software, version 1.8.4, was used to generate Fastq files. The genome sequence was then indexed using the rsem-prepare-reference command.

Each fastq file was trimmed and checked for quality with fastp (v. 0.12.2) and then aligned to the UCSC hg38 human genome using HISAT2 (v.2.1.0)71,72. Transcript counts were extracted using the featureCounts function of the Rsubread package.

QUANTIFICATION AND STATISTICAL ANALYSIS

All statistics were performed using either Graphpad Prism 10 or using R. All data represent the mean ± s.e.m. When only two independent groups were compared, significance was determined by either a two-tailed or one-tailed unpaired t test with Welch's correction. A p value < 0.05 was considered significant; *p < 0.05, **p < 0.01, ***p < 0.001, ****p < 0.0001. The analyses were performed in GraphPad Prism v.10. All experiments were independently performed at least three times with similar results.